CORNELL UNIVERSITY

Center for Radiophysics and Space Research

ITHACA, N. Y.

[redacted]

CRSR 579

SIX-COLOR PHOTOMETRY OF IAPETUS, TITAN, RHEA, DIONE AND TETHYS

M. Noland[1*], J. Veverka[1], D. Morrison[2], D. Chulkshank[2], A. R. Lazarewicz[2], N. D. Morrison[2], L. Elliot[1*], J. Goguen[1*] and J. A. Burns[3*]

[redacted]

SIX-COLOR PHOTOMETRY OF IAPETUS, TITAN, RHEA, DIONE AND TETHYS

M. Noland[1*], J. Veverka[1], D. Morrison[2], D. P. Cruikshank[2], A. R. Lazarewicz[2], N. D. Morrison[2], J. L. Elliot[1*], J. Goguen[1*] and J. A. Burns[3*]

1. Laboratory for Planetary Studies
   Cornell University
   Ithaca, New York 14850

2. Institute for Astronomy
   University of Hawaii
   Honolulu, Hawaii 96822

3. Center for Radiophysics and Space Research
   Cornell University
   Ithaca, New York 14850

* Guest Observer, Mauna Kea Observatory,
University of Hawaii

April, 1974

ABSTRACT

Six-color photometric observations made during Saturn's 1972/73 opposition enable us to separate the solar phase and orbital phase contributions to the observed light variations of Iapetus, Titan, Rhea, Dione and Tethys. Titan shows no orbital variations, but has phase coefficients which range from negligible values in the infrared to 0.014 mag/deg in the ultraviolet. Rhea has a bright leading side, a light curve amplitude of about 0.2 mag, which increases toward short wavelengths, and surprisingly large phase coefficients, which increase from 0.025 mag/deg in the red to 0.037 mag/deg in the ultraviolet. Combined with other available information, this behavior suggests a very porous, texturally complex surface layer. Dione also has a leading side which is a few tenths of a magnitude brighter than the trailing side, but the light curve amplitude has little wavelength dependence and the phase coefficients are significantly smaller than those of Rhea, suggesting a less intricate surface texture. The leading side of Tethys is probably a few tenths of a magnitude brighter than the trailing side. Our Iapetus observations generally supplement the earlier work by Millis. The phase coefficients of the bright (trailing) side are typically $\sim$ 0.03 mag/deg and are not strongly wavelength dependent; the dark (leading) side coefficients are large ($\sim$ 0.05 mag/deg) and increase at shorter wavelengths, indicating a very porous and intricate surface texture.

The light curve amplitude shows a slight increase at shorter wavelengths, suggesting an increasing contrast between the dark and bright materials. The spectral reflectance curves we derive for the satellites are in agreement with the spectrophotometry of McCord, Johnson, and Elias.

1.) Introduction

Previous photometric observations of the satellites of Saturn have been insufficient to permit a clear separation of the solar phase and orbital phase contributions to the observed light variations. The former quantity gives information on the surface microstructure of bodies without atmospheres, while the latter quantity yields information on the global distribution of albedo features, which in some cases may be related to interactions between the satellite and its environment. In order to determine the solar and orbital phase coefficients and to establish their wavelength dependence, we undertook a program of six-color photometry of Iapetus, Titan, Rhea, Dione and Tethys during Saturn's 1972/1973 apparition. The observations cover solar phase angles from +6.4° to -4.8° and wavelengths from 0.35 to 0.75μm.

2.) Observations

The observations were made with the 61-cm telescope and standard photoelectric photometer of the Mauna Kea Observatory. This photometer uses an EMI 9558B (S-20) photomultiplier, thermoelectrically cooled to -20°C, together with photon-counting electronics and teletype data recording. We observed in six colors: the standard four Strömgren filters (u, v, b, y), an interference filter centered at 6239 Å (here called the r' filter), and a wideband Schott RG 715 (here called the i'filter) that, in combination with the photomultiplier, provided a broad passband between 0.7 and 0.8μm. The central wavelengths and bandwidths of these filters are given in Table 1.

Each observation normally consisted of three consecutive integrations in each of the six colors, followed by measurements of the sky. The integration times were 8 seconds for standard stars, either 8 or 16 seconds for Titan, and 16 seconds for the other satellites. An aperture 15 arcseconds in diameter was most suitable for the outer satellites (Iapetus, Titan, and sometimes Rhea). For the inner satellites, however, the high background level of light scattered from Saturn necessitated the use of a 7-arcsecond aperture. Standard stars were observed approximately once per hour, usually with both the 15- and 7-arcsecond apertures.

For Iapetus and the standard stars, the sky signal was measured by simply offsetting the telescope north or south by 15 to 20 arcseconds. A more careful procedure was required for the inner satellites, however, in which the sky was measured on both sides of the satellite at the same radial distance from Saturn as the satellite. Errors in positioning the aperture in the presence of a strong gradient in the scattered light are the source of most of the uncertainty in the measurements of Dione, and especially of Tethys. A discussion of these effects, together with a plot of scattered light as a function of distance from Jupiter obtained with this same telescope and photometer, has been presented by Cruikshank and Murphy (1973).

For each observation we averaged the number of counts, computed a standard deviation, and subtracted the average of the sky readings. Where several sequences were taken on the same satellite within a short period of time, all of these measurements were combined to generate a single 6-color set of observations.

Numerous observers have measured extinction in the uvby system at Mauna Kea and have demonstrated that the mean coefficients are highly reproducible (Wolff and Wolff 1971; Morrison et al. 1973). The uvby extinction coefficients that we measured for our standard comparison star (37 Tau = HR 1256)generally agreed with the mean values (Table 1).

For the r' and i' filters, we determined extinction coefficients of .09 ± .02 and .07 ± .02 mag/airmass, respectively. Since we did not normally observe at airmasses greater than 2 and we reduced the magnitudes relative to 37 Tau, the uncertainties in these coefficients are insignificant.

Differential magnitudes, expressed relative to our primary standard, 37 Tau, are sufficient for the determination of phase coefficients and amplitudes of light curves. These magnitudes, reduced to mean opposition distance from Earth and Sun ($r = 9.54$ AU and $\Delta = 8.54$ AU), are tabulated in Tables 2 to 6. In a later section, we will derive a transformation between our instrumental y-magnitudes and the V-magnitudes of the UBV system and between our instrumental colors and those of the standard uvby system. However, since these transformations introduce uncertainties in addition to those inherent in the basic differential photometry, we will base most of our physical conclusions on the instrumental relative values.

Estimates of the uncertainty in each satellite magnitude (relative to 37 Tau) can be obtained in at least two ways. First, we compute the internal standard error obtained in averaging the three or more integrations that make up each observation point. Second, observations made during the same night at similar solar and orbital phase angles can be checked for consistency. For the inner satellites, the errors estimated in the second way

are usually greater than the internal errors, a result in agreement with our expectation that the main source of uncertainty is the non-reproducibility of the sky readings. The larger of the two errors is adopted for each point and quoted in the tables.

3.) Method of Analysis

Mean opposition magnitudes of the satellites relative to 37 Tau are given in Tables 2 to 6. Assuming the magnitudes vary linearly with solar phase angle and sinusoidally with orbital phase angle, we perform a four-parameter least-squares fit to the data for each satellite with the equation:

$$M = M_o + \beta\alpha + \mu_o \sin(\theta - \theta_o) \qquad (1)$$

where M_o = mean magnitude relative to 37 Tau

α = solar phase angle

β = phase coefficient

θ = orbital phase angle, measured in the prograde sense from superior conjunction

θ_o = orbital phase angle at which M_o occurs

and $2\mu_o$ = peak to peak amplitude of the orbital phase variation.

Except in the case of Tethys, points are weighted as $1/\sigma^2$, where σ is the error assigned to an individual point according to the procedure outlined in Section 2. In the case of Tethys a more subjective weighting procedure is used (see Section 7).

Note that, because of our interest in the wavelength dependence of phase coefficients and amplitudes, we reduce the magnitudes from each filter separately. Separate fits to colors

are not attempted except for the case of Iapetus (Morrison et al., 1974b).

Several assumptions and approximations are implicit in Eq. (1). First, a linear dependence on the solar phase angle is assumed, whereas over the range of phase angles of interest (0° to 6°) opposition effects are important for dark, texturally complex surfaces, and a dependence of the phase coefficient on phase angle can be expected. Secondly, the orbital variation assumes that the period of rotation of the satellite equals its orbital period. This assumption seems to be well founded, and only in the case of Tethys has it been questioned (Franz and Millis, 1973). Finally, the orbital sinusoid is only the first term in the general expansion of the brightness variation, and, in fact, the brightness, not the magnitude, is the quantity which varies sinusoidally with orbital phase. Only when $\Delta M \lesssim 0.3$ mag is it true that

$$\Delta M_{\alpha=0} = -2.512 \log \left(1 - \frac{\mu_1 \sin\theta}{I_o}\right) \approx 1.1 \frac{\mu_1 \sin\theta}{I_o} \equiv \mu_o \sin\theta$$

where μ_1 = half amplitude of the brightness variation and I_o = brightness at $\theta = 0°$ and 180° for $\alpha = 0°$ (see Section 8). For Iapetus this approximation is invalid, and the brightness version of Eq. (1) must be used.

The philosophy adopted here is to regard Eq. (1), or its brightness equivalent in the case of Iapetus, as a suitable starting point for our analysis. For each satellite we shall determine the four parameters from the data and then comment upon the meaning and validity of the solutions in each particular case.

4.) Titan

When the thirty available observations (Table 2) are fitted for all four parameters in Eq. (1), it is found that the light curve amplitude ($2\mu_o$) is less than 0.02 mag at all wavelengths, in agreement with the earlier observations by Harris (1961), Blanco and Catalano (1971) and McCord, Johnson and Elias (1971).

Since there is no observable orbital variation, the data may be analyzed by means of a two-parameter fit

$$M = M_o + \beta\alpha$$

to determine the wavelength dependence of the phase coefficients. The results, shown in Table 7 and Figs. 1 and 2, range from 0.014 mag/deg in the ultraviolet to negligible values in the infrared. The only previous determination of a phase coefficient for Titan is that of Blanco and Catalano (1971). Although these authors fit their data to a quadratic expression for α, a linear equation yields an equally good fit with $\beta(V) = 0.006 \pm 0.001$ mag/deg, a result in agreement with our y value.

Recent models of Titan (Pollack, 1973; Danielson *et al.*, 1973; Veverka, 1973; Barker and Trafton, 1974)

postulate various amounts of atmosphere and aerosols on Titan. Some involve optically thick clouds, while others require only a thin aerosol haze over a partially obscured surface. The ability of these models to reproduce the observed phase coefficients is discussed in detail in Noland and Veverka (1974).

5.) Rhea

For Rhea and the inner satellites sky brightness measurements become progressively more difficult, with the result that certain measurements are noticeably discrepant and have to be excluded. There remain 17 measurements made with the 15-arcsecond aperture and up to 30 measurements (depending on the filter) made with the 7-arcsecond aperture (Table 3). No systematic difference between the two sets is evident, and they have been combined to determine the parameters given in Table 8.

A sinusoidal variation in magnitude with an amplitude of about 0.2 mag provides a good fit to the data (Fig. 3). The rotation period appears to be completely synchronous, with maximum brightness occuring near $\theta = 90°$ and minimum brightness near $\theta = 270°$. It is therefore the leading side of Rhea which is brighter. These results are in agreement with earlier, less comprehensive measurements by Harris (1961), McCord, Johnson and Elias (1971), Blanco and Catalano (1971), and Blair and Owen (1974).

In Fig. 4 we plot the derived light curve amplitude and phase coefficient against wavelength. The amplitude shows a sharp rise at wavelengths less than 0.5μm. This behavior can be explained by a two-component model of the surface in which the relative contrast between the dark and bright areas increases strongly shortward of 0.5μm.

The spectral reflectance data of McCord et al. (1971) show that, relative to the (trailing side)/(leading side) contrast ratio at 0.56μm, the trailing (dark) side is darker than the leading side at shorter wavelengths, in agreement with our results, and possibly brighter at longer wavelengths, where our results are inconclusive. Such an effect can be explained if the spectral reflectance of the brighter material is flat over the wavelength range of interest (consistent with ice), while the spectral reflectance of the darker material increases from ultraviolet to red (consistent with carbonaceous or silicate material).

The value of the phase coefficient increases from 0.025 mag/deg in the red to 0.037 mag/deg in the ultraviolet. We reiterate that these are linear coefficients, determined at small phase angles, where opposition effects are likely to be important, and that any comparison with phase coefficients of other bodies, determined at larger phase angles, must be made judiciously (see, for example, Morrison et al., 1974b). Nevertheless, Rhea's phase coefficients are large, and these high coefficients, coupled with the very high geometric albedo in the visible (0.6-0.8 according to Morrison, 1974), imply a very porous and texturally complex surface layer. Such a surface layer is also needed to explain the relatively deep negative branch in the polarization curve of Rhea found by Zellner (1972).

6.) Dione

The available data are given in Table 4 and plotted in Fig. 5. All measurements were made with the 7-arcsecond aperture.

The data are fitted in two ways:

1. Using a four parameter fit, as before.
2. Assuming $\theta_o = 0°$ at all wavelengths, and solving for three parameters only.

The parameters obtained by both methods are given in Table 9. Since the first method yields inconsistent values of θ_o ranging from -21° (or 339°) to +34°, the assumption used in the second method appears justified. The main advantage of the second method is that more reasonable values of β and μ_o in the $\underline{u}$ are obtained. In what follows we will adopt the method (2) solution.

The leading side of Dione is clearly brighter than the trailing side, consistent with the more fragmentary results of McCord, Johnson, and Elias (1971) and with the recent photometry of Franz and Millis (1973) and Blair and Owen (1974). It is also clear, however, that our sinusoidal fit to the data is not a very good one. Since the amplitude of the light curve appears to be larger between 180° and 360° than between 0° and 180°, the amplitudes of 0.2 to 0.3 mag indicated in Table 9 may be underestimates. The measurements of Franz and Millis, for example, suggest an amplitude closer to 0.4 mag, and Blair and Owen claim an amplitude of 0.8 mag.

Unfortunately, we have too few data points to justify separate fits to the two sides.

Within the error bars there is no wavelength dependence to the derived light curve amplitudes. Unlike Rhea, Dione does not show a strongly wavelength-dependent contrast between the dark and bright areas. McCord et al. (1971) report similar findings.

Not much weight should be given to the precise values of the phase coefficients for Dione since the errors involved are large -- a fact underscored by the unphysical negative values of β found in the i' filter. Nevertheless, the coefficients for Dione are significantly smaller than those for Rhea. The smaller phase coefficients and the comparable goemetric albedo (0.6) given by Morrison (1974) indicate that Dione probably has a less intricate surface texture than Rhea.

7.) Tethys

The observations of Tethys given in Table 5 are very noisy due to scattered light from Saturn. They are analyzed by the two methods used in the case of Dione, with the most reproducible points weighted as 1, and all others (whose reproducibility is bad or uncertain) weighted as 1/4. Since method (1) gives values of θ_o ranging from -41° (319°) to +54°, we adopt the method (2) solution, which sets θ_o = 0° at all wavelengths. The derived parameters are shown in Table 10, and a typical curve is given in Fig. 6.

The leading side of Tethys is probably brighter than the trailing side. The formal values of the light curve amplitudes lie between 0.1 and 0.2 mag, which is not inconsistent with the results of Blair and Owen (1974), Franz and Millis (1973), and McCord et al. (1971). However, Fig. 6 indicates that amplitudes up to 0.5 mag cannot be excluded. The phase coefficients are comparable to those for Dione, but, again, the uncertainties are large.

Finally, since our Tethys observations extend over only two months, we cannot test the validity of the slightly non-synchronous rotation period suggested by Franz and Millis (1973).

8.) Iapetus

The basic data are given in Table 6, and the b filter magnitudes, uncorrected for solar phase effect, are plotted against orbital phase angle in Fig. 7. It is clear that: 1) $\theta_o \simeq 0°$ (in fact, for all filters Eq. (1) yields $\theta_o = 0° \pm 2°$) and 2) $2\mu_o \simeq 2$ mag (which renders Eq. (1) inapplicable, as noted in Section 3). Accordingly, we assume $\theta_o = 0°$ and solve Eq. (1), written in terms of brightness:

$$M = M_o + \beta\alpha - 2.512 \log [1 - \mu_2 \sin\theta] \qquad (2)$$

for three parameters: M_o, β and μ_2. Here $\mu_2 \equiv \mu_1/I_o$, where μ_1 = half amplitude of the brightness variation and I_o = brightness at $\theta = 0°$ and 180°. It should also be noted that Widorn (1952) found a good fit to the then available Iapetus measurements by using the equation:

$$I = 0.571 - 0.429 \sin\theta.$$

The form of this expression is equivalent to (2) if solar phase angle effects are ignored.

The result of fitting the whole light curve to Eq. (2) is shown in Fig. 8 for the b filter. We find M_o (b) = 6.28 ± 0.2 mag (relative to 37 Tau) and $\beta = 0.025 \pm 0.005$

mag/deg, but the agreement between the curve and the data points is not very good near $\theta = 90°$ or 270°. For an improved fit, we must analyze the two sides of Iapetus separately.

The analysis of the bright side yields a very good fit to the observations with the parameters shown in Table 11. Note that in this table the magnitude equivalent of μ_2 is given. For the b filter the bright side value of M_o is about 0.1 mag greater than the value obtained by fitting the whole light curve, but the value of the phase coefficient is about the same in the two cases. A similar situation holds for the parameters obtained with the other filters.

If Eq. (2) is applied to the dark side, the formal fit yields negative values of β with large uncertainties and correspondingly large values of M_o. The reason for this unphysical situation is clear: since the range of dark side observations is limited to phase angles between 4.0° and 5.6°, a wide range of β's will give statistically equally valid fits. The range of acceptable β's for the dark side can be limited, however, by making the reasonable requirement that

$$M_o \text{ (dark side)} = M_o \text{ (bright side)}.$$

Since the M_o for the bright side is well determined (see above), the dark side analysis can be reduced to a two-

parameter fit for β and μ_2. The results are shown in Fig. 9 and Table 11, where the total light curve amplitude $\mu_2 = \mu_2$ (dark) + μ_2 (bright) is also given.

The wavelength dependence of the phase coefficients is shown in Fig. 10. Our phase coefficients for the dark side are large ($\sim$ 0.05 mag/deg) and wavelength dependent, with the larger values occurring at shorter wavelengths. Although these are the best values for the dark side, they should be treated with caution, for changing M_o by 0.1 mag changes β by about 0.015 mag/deg. The phase coefficients for the bright side are smaller ($\sim$ 0.03 mag/deg) and not noticeably wavelength dependent. These results agree well with the earlier work of Millis (1972), who found the phase coefficients for the dark and bright sides to be 0.06 and 0.02 mag/deg, respectively, in the visible.

The unusually large values of β for the dark side are consistent with a very low albedo for this side (0.04 to 0.05 according to Murphy et al., 1972 and Morrison, 1973) and with the deep negative branch of the polarization curve (Zellner, 1972), all of which point to a very porous and intricate surface texture. The lower values of the phase coefficient on the bright side are consistent with a brighter surface, a less porous surface, or both.

The light curve amplitudes for the dark and bright sides of Iapetus are plotted against wavelength in Fig. 11, along with the total amplitude. Since the brighter

material dominates the average photometric behavior of the surface, it is not surprising that the bright side amplitude, which is a measure of the bright/average spectral reflectance ratio, appears to be wavelength independent. The dark side and total amplitudes increase slightly towards the blue, suggesting that the contrast between the dark and bright materials increases towards shorter wavelengths. Morrison et al. (1974b) show that, in fact, the spectral reflectance of the bright material is fairly flat, while the spectral reflectance of the dark material increases with wavelength.

A great deal of additional physical information about Iapetus can be obtained from a comparison of light curves at different values of the tilt of the Saturn system and, especially, from simultaneous photometric and radiometric light curves. Such analyses, based in part on the observations presented here, are to be found in Morrison et al. (1974b). In that paper are derived values for the radius, the distribution of geometric albedo on the satellite, and the mean bolometric Bond albedo and mean phase integral for the bright (trailing) side.

9.) V Magnitudes, colors, and albedos

Up to this point, we have considered only differential magnitudes and colors, expressed on the instrumental system. We now discuss the transformation to the standard system and derive absolute V magnitudes and colors for the satellites.

On most nights, we observed, in addition to the satellites and 37 Tau (HR 1256), at least two additional standards, one of which was usually 47 Tau (HR 1311). On two nights in January, however, we performed a complete transformation, using seven uvby standards. The V magnitudes and colors of a number of standard stars are listed in Table 12, together with the mean V magnitudes and colors of the satellites (taken from Tables 7 to 11), transformed to the standard system. For the transformation of the satellite magnitudes and colors, we used the mean of transformation coefficients obtained on seven nights in December and January. The errors introduced in the transformation could be as great as $\pm$ 0.02 in V, although an examination of the residuals for the standard stars on the two nights on which the transformation was performed suggests that the standard error in V is probably only $\pm$ 0.01 magnitude. The uncertainties in the colors are less than $\pm$ 0.01 magnitude. Since none of these satellites exhibits large variations in color, the transformation applied to the mean magnitudes and colors should apply equally well to the individual measurements.

No standard system exists for the r' and i' filters, so we adopt our instrumental system as the standard and define the zero points of the color indices so that $(r' - y) = (i' - y) \equiv 0$ for 37 Tau. The mean values of these color indices for the standard stars and satellites are also given in Table 12.

The mean V magnitudes of the satellites derived from our measurements are compared with those obtained by other authors in Table 13. For Titan, the excellent agreement with the magnitude obtained by Blanco and Catalano (1971) and the difference of 0.05 magnitude from that obtained by Harris (1961) are similar to the agreement between Mauna Kea magnitudes and those published by Harris and by Blanco and Catalano for the Galilean satellites (Morrison et al., 1974a). For the other satellites, our V magnitudes are consistently brighter than those published previously. These differences probably result from the fact that we obtain magnitudes at phase angle $\alpha = 0°$ using derived phase coefficients, whereas previous observors did not correct their magnitudes for dependence on phase angle.

In order to determine the spectral reflectance of the satellites from the colors given in Table 12, we must know the colors of the Sun in our photometric system. Morrison et al. (1974a) have derived the solar values of the three color indices of the uvby system from a comparison of the published spectrophotometry of seven

uvby standard stars with the solar spectral energy distribution measured by Arvesen et al. (1969). We will now use a similar approach to derive the (r' - y) and (i' - y) colors of the Sun.

For three of the secondary standards observed in this program - 64 Tau, 68 Tau, and ρ Gem - spectral energy distributions have been published by Code (1960) or Oke and Conti (1966). We have adjusted these distributions to be on the scale defined for Vega by Oke and Schild (1970). The solar energy distribution published by Arvesen et al. (1969) yields irradiance ratios in our filters of r'/y = 0.902 and i'/y = 0.679. Table 14 gives the color indices derived for the Sun from the observations of these 3 standards. We also derive two independent calibrations of the colors of the Sun from our measurements of o Vir and 29 Psc and the ratios of the irradiance of these stars to that of the Sun obtained by Johnson (1971) and Chapman et al. (1973), respectively. Results for these two stars are also given in Table 14. We take a straight average to obtain the final color indices of the Sun, which are given in Table 15 along with the uvby color indices derived by Morrison et al. (1974a). The uncertainties given are based on the uncertainties in the stellar observations but do not include an additional uncertainty of perhaps ± 0.05 magnitude due to possible errors in the energy distributions of the Sun (Arvesen et al., 1969) and of Vega (Oke and Schild, 1970).

Also listed in Table 15 are the mean colors of the satellites, relative to the Sun, and the corresponding

albedos, normalized to unity for the y filter (0.55μm). These albedos are plotted as a function of wavelength in Figure 12, together with the UBV colors obtained by Harris (1961) and the spectrophotometric colors of McCord et al. (1971).

The agreement among the three sets of data is quite good, except for Harris' long wavelength data, which may be contaminated by light from Saturn or its rings (McCord et al., 1971). The Titan reflectance curve displays its well-known ultraviolet dip. We also note the remarkable similarity in the colors of Rhea, Dione, Tethys, and Iapetus. (Although we have plotted the mean reflectance for Iapetus, the high-albedo material is the source of most of the reflected light).

10.) Conclusion

The extensive photometric observations of Titan, Iapetus, Rhea, Dione and Tethys presented in this paper have made it possible to separate the solar phase and orbital phase contributions to the observed light variations of these satellites.

For Titan, we have obtained the wavelength dependence of its solar phase coefficient. This dependence should prove useful in constructing future model atmospheres.

The other four satellites show a surprising array of different photometric behaviors. Rhea and Dione have similar high albedos, but differ in their phase coefficients

and in the wavelength dependence of their light curve amplitudes. Rhea and the bright side of Iapetus have similar phase coefficients, but they differ strongly in albedo. The inner satellites have bright leading sides and light curve amplitudes of a few tenths of a magnitude, while Iapetus has a dark leading side and an amplitude of almost two magnitudes. Despite these differences, all four satellites have similar spectral reflectivities. Clearly Iapetus, Rhea, Dione and Tethys are complex objects, varying substantially from one another in surface structure and/or composition.

Acknowledgment

We wish to thank T. V. Johnson, F. Franklin, and C. Chapman for helpful comments and discussions and the entire staff of the Mauna Kea observatory for their assistance. This work was supported in part by NASA Grants NGR-033-010-082 and NGL-12-001-057.

References

Arvesen, J. C., Griffin, R. N., and Pearson, B. D. (1969). Determination of extraterrestrial solar spectral irradiance from a research aircraft. Applied Optics 8, 2215-2232.

Barker, E. S., and Trafton, L. M. (1974). Ultraviolet reflectivity and geometrical albedo of Titan. Icarus 20, 444-454.

Blair, G. N., and Owen, F. N. (1974). The UBV orbital phase curves of Rhea, Dione, and Tethys. Icarus 22, 000-000.

Blanco, C., and Catalano, S. (1971). Photoelectric observations of Saturn satellites Rhea and Titan. Astron. Astroph. 14, 43-47.

Chapman, C. R., McCord, T. B., and Johnson, T. V. (1973). Asteroid spectral reflectivities. Astron. J. 78, 126-140.

Code, A. D. (1960). Stellar energy distribution. In "Stellar Atmospheres" (ed. J. L. Greenstein), University of Chicago, Chicago, pp. 50-87.

Cruikshank, D. P., and Murphy, R. E. (1973). The post-eclipse brightening of Io. Icarus 20, 7-17.

Danielson, R. E., Caldwell, J. J., and Larach, D. R. (1973). An inversion in the atmosphere of Titan. Icarus 20, 437-443.

Franz, O. G., and Millis, R. L. (1973). UBV photometry of Enceladus, Tethys, and Dione. Bull. American Astron. Soc. 5, 304.

Harris, D. L. (1961). Photometry and polarimetry of planets and satellites. In "Planets and Satellites" (ed. by G. P. Kuiper and B. M. Middlehurst), University of Chicago, Chicago, pp. 272-342.

Johnson, T. V. (1971). Galilean satellites: Narrowband photometry 0.30 to 1.10 microns. Icarus 14, 94-111.

McCord, T. B., Johnson, T. V., and Elias, J. H. (1971). Saturn and its satellites: Narrow-band spectrophotometry (0.3-1.1μ). Astrophys. J. 165, 413-424.

Millis, R. L. (1973). UBV photometry of Iapetus. Icarus 18, 247-252.

Morrison, D. (1973). Determination of radii of satellites and asteroids from radiometry and photometry. Icarus 19, 1-14.

Morrison, D. (1974). Albedos and densities of the inner satellites of Saturn. Icarus 22, 000-000.

Morrison, D., Murphy, R. E., Cruikshank, D. P., Sinton, W. M., and Martin, T. Z. (1973). Evaluation of Mauna Kea, Hawaii, as an observatory site. P.A.S.P. 85, 255-267.

Morrison, D., Morrison, N. D., and Lazarewicz, A. R. (1974a). Four-color photometry of the Galilean satellites. Submitted to Icarus.

Morrison, D., Jones, T. J., Cruikshank, D. P., and Murphy, R. E. (1974b). The two faces of Iapetus. In preparation.

Murphy, R. E., Cruikshank, D. P., and Morrison, D. (1972). Radii, albedos, and 20-micron brightness temperatures of Iapetus and Rhea. Astrophys. J. 177, L93-L95.

Noland, M., and Veverka, J. (1974). In preparation.

Oke, J. B. and Conti, P. S. (1966). Absolute spectrophotometry of stars in the Hyades. Astrophys. J. 143, 134-145.

Oke, J. B., and Schild, R. E. (1970). The absolute spectral energy distribution of alpha Lyrae. Astrophys. J. 161, 1015-1023.

Pollack, J. B. (1973). Greenhouse models of the atmosphere of Titan. Icarus 19, 43-58.

Veverka, J. (1973). Titan: polarimetric evidence for an optically thick atmosphere? Icarus 18, 657-660.

Wolff, R. J., and Wolff, S. C. (1971). uvby photometry of Ap stars: the nature of the light variations. Astron. J. 76, 422-430.

Widorn, Th. (1952). Der Lichtwechsel des Saturn Satelliten Iapetus im Jahre 1949. Mitt. Univ.-Sternw. Wien 5, 19-29.

Zellner, B. (1972). On the nature of Iapetus. Astrophys. J. 174, L107-L109.

Figure Captions

Figure 1: Magnitude of Titan as a function of the solar phase angle, α. The meaning of the error bars is discussed in Section 2. All magnitudes in this and subsequent figures are reduced to mean opposition (r = 9.54 AU; Δ = 8.54 AU).

Figure 2: Wavelength dependence of Titan's phase coefficient.

Figure 3: Orbital magnitude variations of Rhea with solar phase angle effects removed. The fitted sinusoidal variation provides an adequate representation of the data.

Figure 4: Wavelength dependence of Rhea's light curve amplitude (top) and phase coefficient (bottom).

Figure 5: Orbital magnitude variations of Dione with solar phase angle effects removed. The sinusoidal fit appears to underestimate the light curve amplitude near θ = 270°. This difficulty is discussed in Section 6.

Figure 6: Orbital magnitude variation of Tethys in the y filter with solar phase angle effect removed. The sinusoidal fit is not good, as noted in Section 7.

Figure 7: Magnitude variation of Iapetus in the b filter, uncorrected for solar phase angle effect.

Figure 8: Orbital magnitude variation of Iapetus in the b filter with solar phase angle effect removed. Since such a fit is unsatisfactory near $\theta = 90°$, the two sides of Iapetus must be analyzed separately.

Figure 9: Orbital magnitude variations of Iapetus with solar phase angle effects removed, obtained by analyzing the data for the bright side ($0° \leq \theta \leq 180°$) and for the dark side ($180° \leq \theta \leq 360°$) separately (see Section 8).

Figure 10: Wavelength dependence of the phase coefficients of Iapetus for:

a) the bright side

b) the dark side.

Figure 11: Wavelength dependence of the light curve amplitude of Iapetus:

a) bright side only

b) dark side only

c) combined amplitude.

Figure 12: Wavelength dependence of the geometric albedos of Titan, Rhea, Dione, Tethys and Iapetus (at $\theta = 0°$), normalized at 0.55μm (y filter). Measurements by Harris (1961) and McCord et al. (1971), similarly normalized, are shown for comparison.

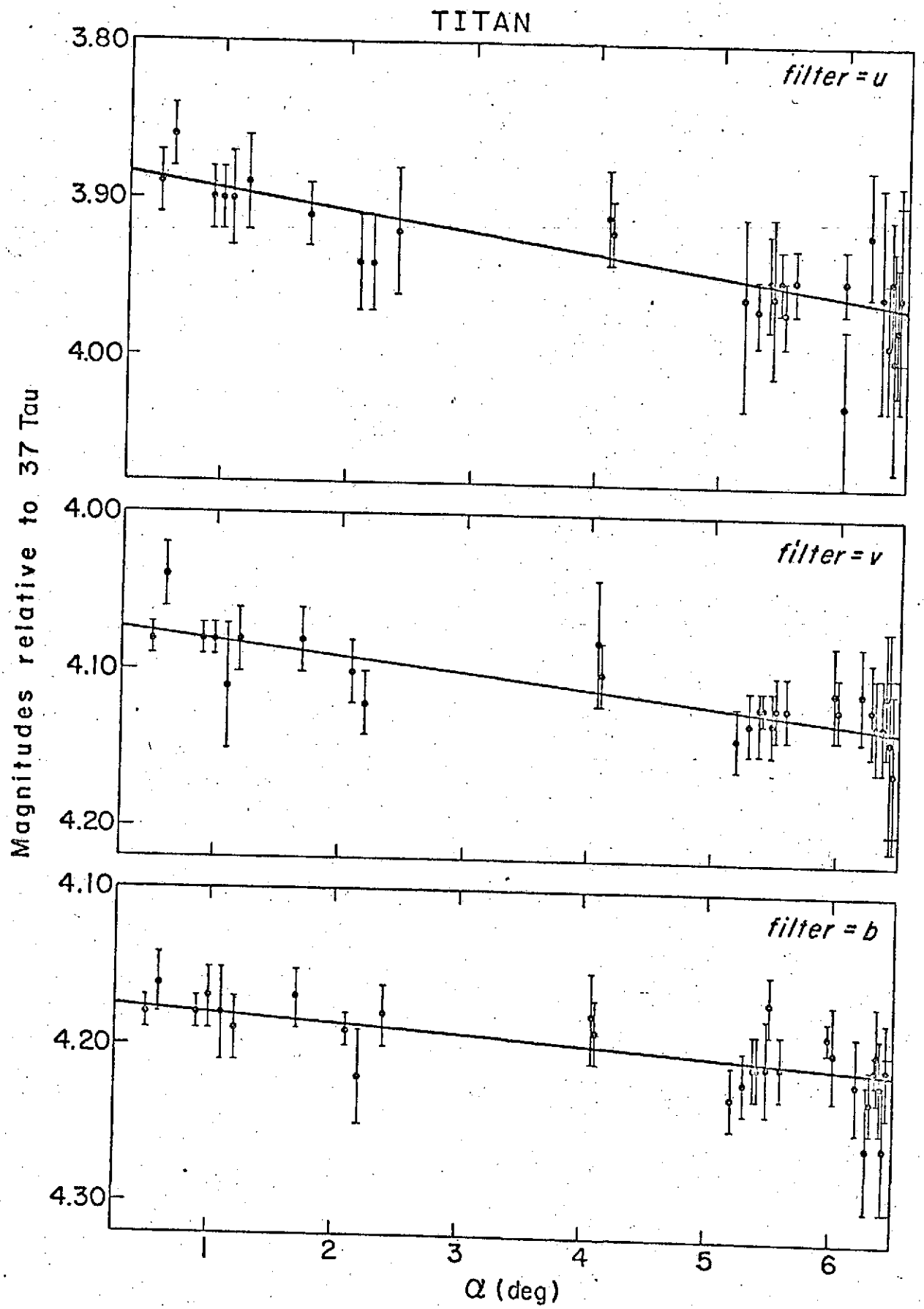
TITAN
filter = u
filter = v
filter = b
3.80
3.90
4.00
4.00
4.10
4.20
4.10
4.20
4.30
Magnitudes relative to 37 Tau
1
2
3
4
5
6
α (deg)

Figure 1.

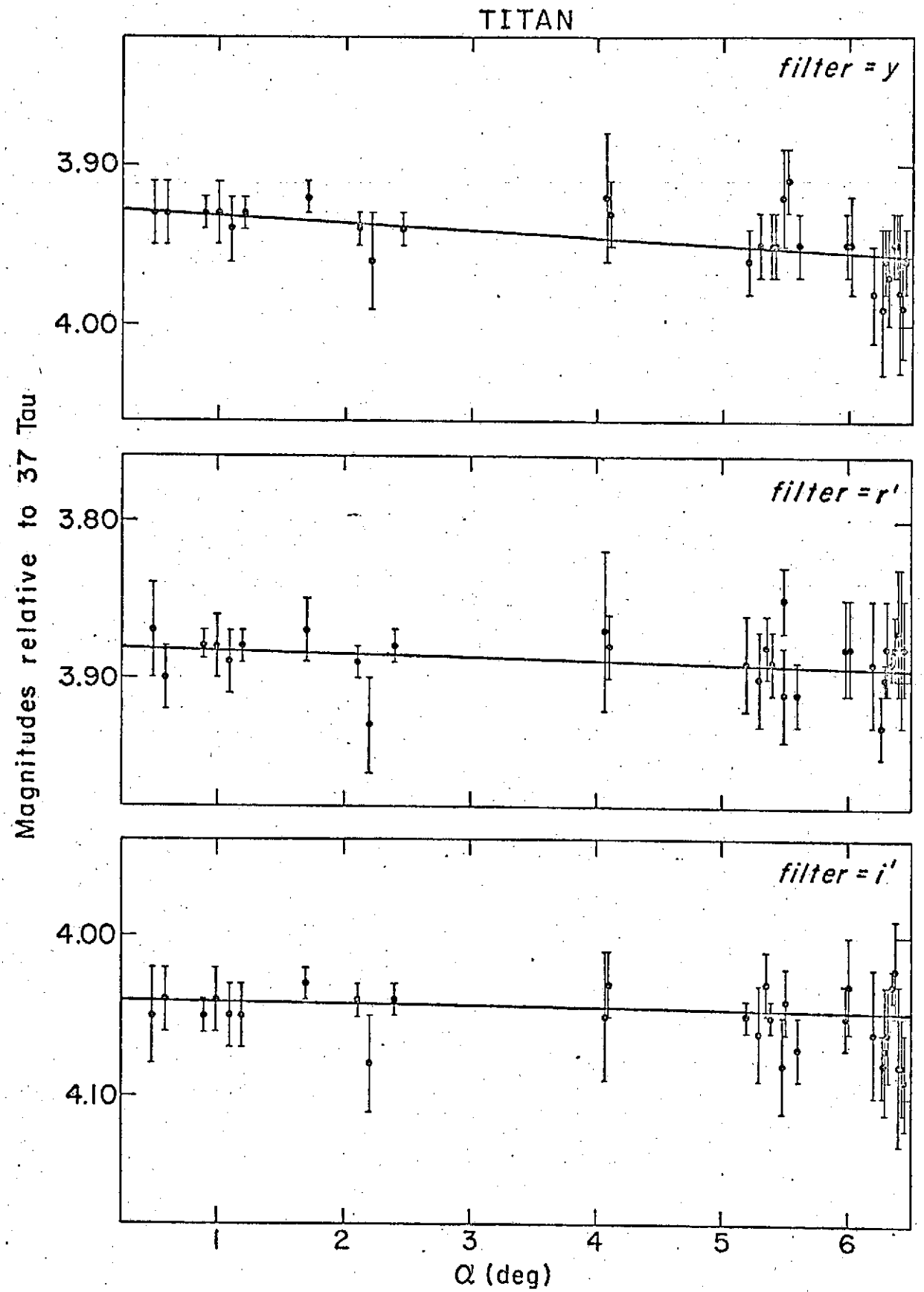
TITAN
filter = y
filter = r'
filter = i'
3.90
4.00
3.80
3.90
4.00
4.10
Magnitudes relative to 37 Tau
1
2
3
4
5
6
α (deg)

Figure 1a.

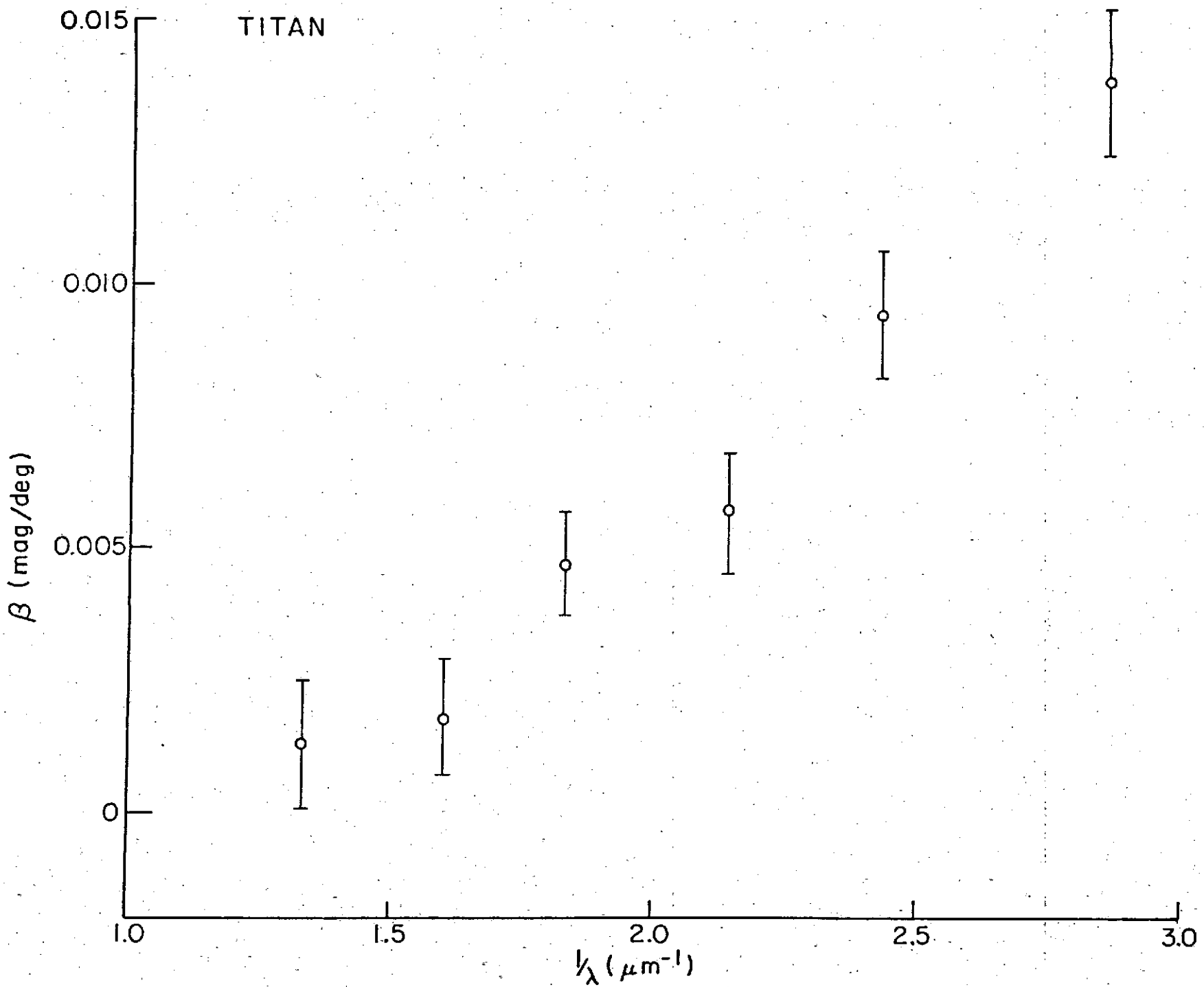

Figure 2.

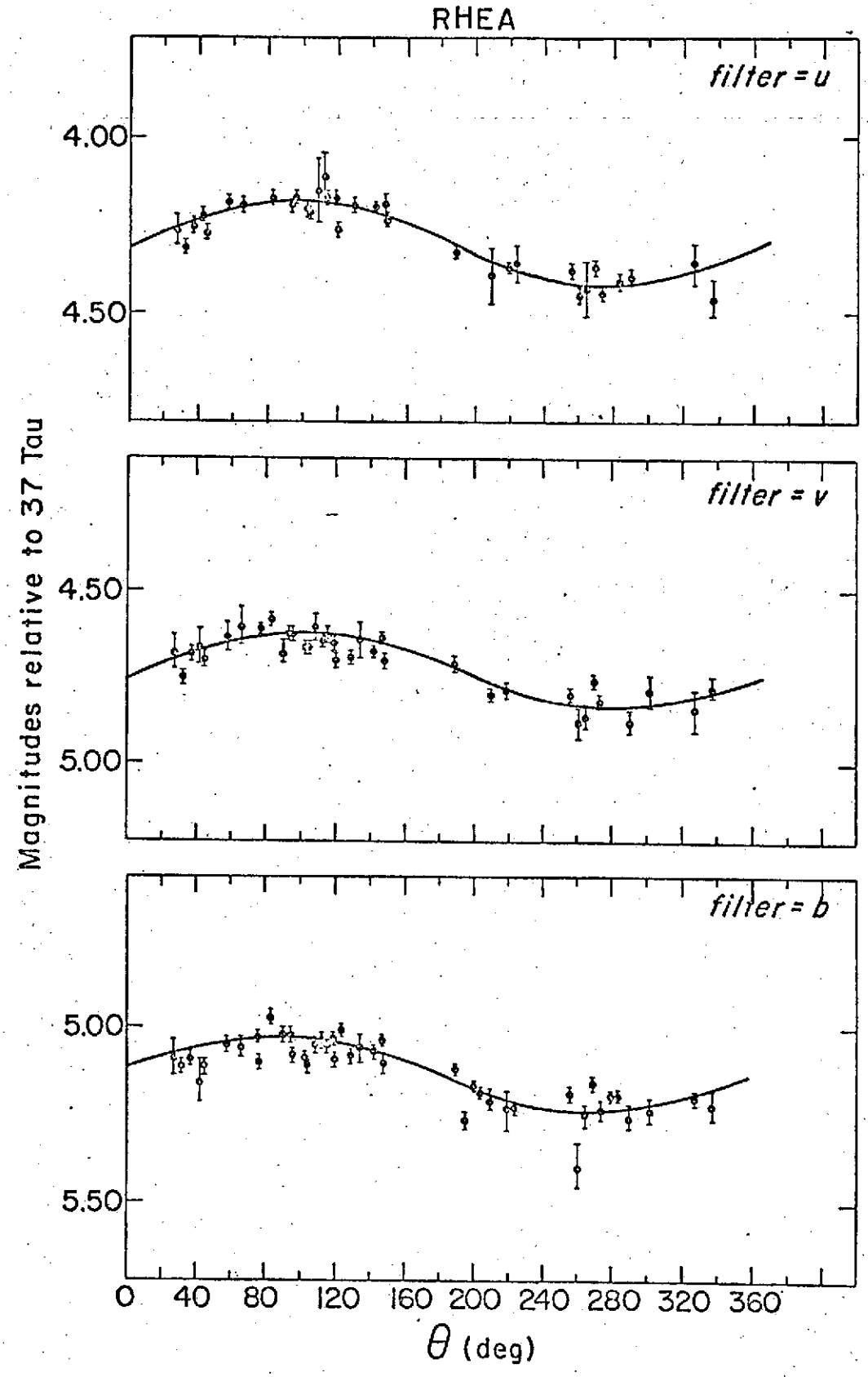
RHEA
filter = u
filter = v
filter = b
4.00
4.50
4.50
5.00
5.00
5.50
Magnitudes relative to 37 Tau
0
40
80
120
160
200
240
280
320
360
θ (deg)

Figure 3.

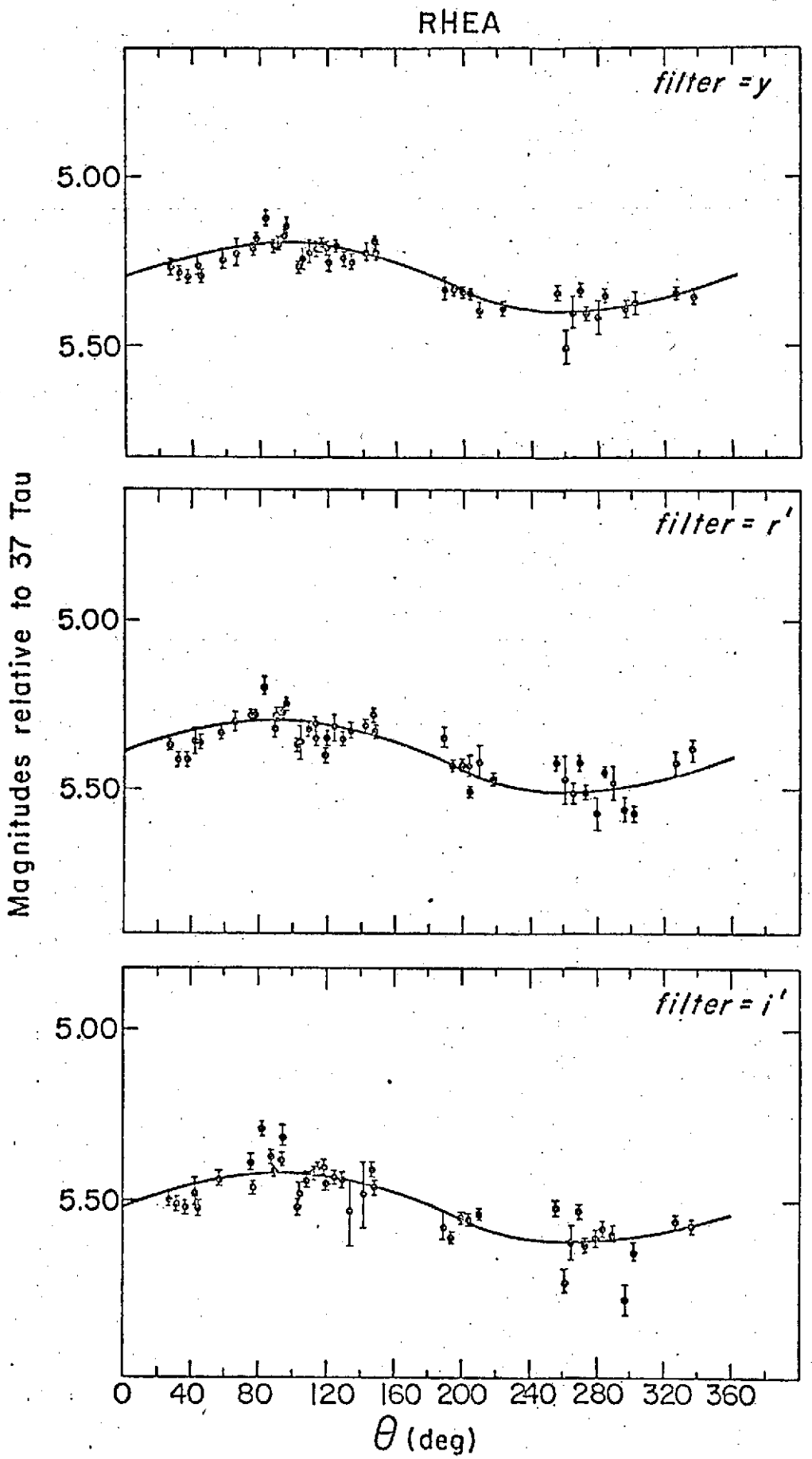
RHEA
filter = y
filter = r'
filter = i'
5.00
5.50
Magnitudes relative to 37 Tau
0
40
80
120
160
200
240
280
320
360
θ (deg)

Figure 3a.

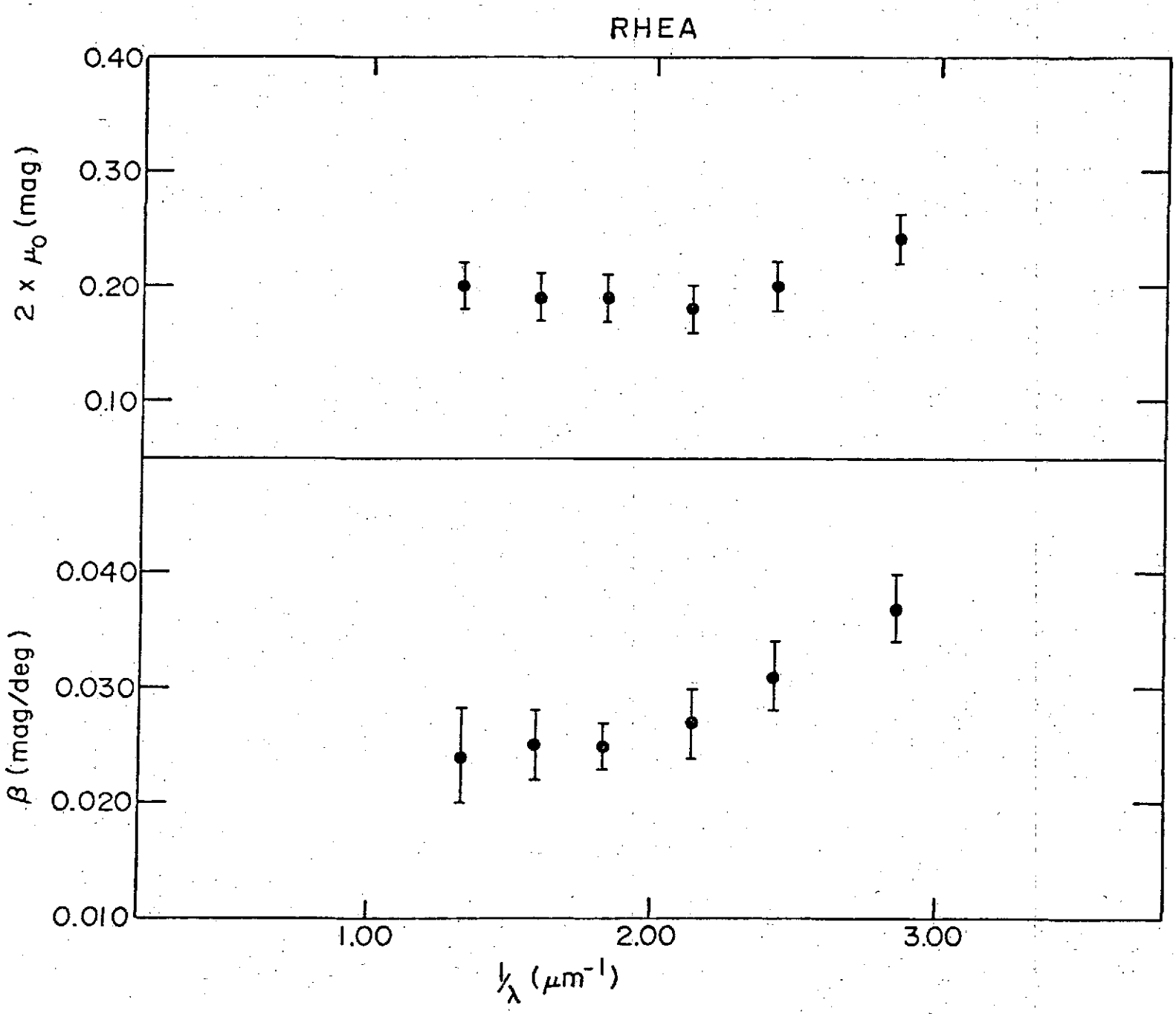
RHEA
0.40
0.30
0.20
0.10
2 x μ_0 (mag)
0.040
0.030
0.020
0.010
β (mag/deg)
1.00
2.00
3.00
$1/\lambda$ (μm^{-1})

Figure 4.

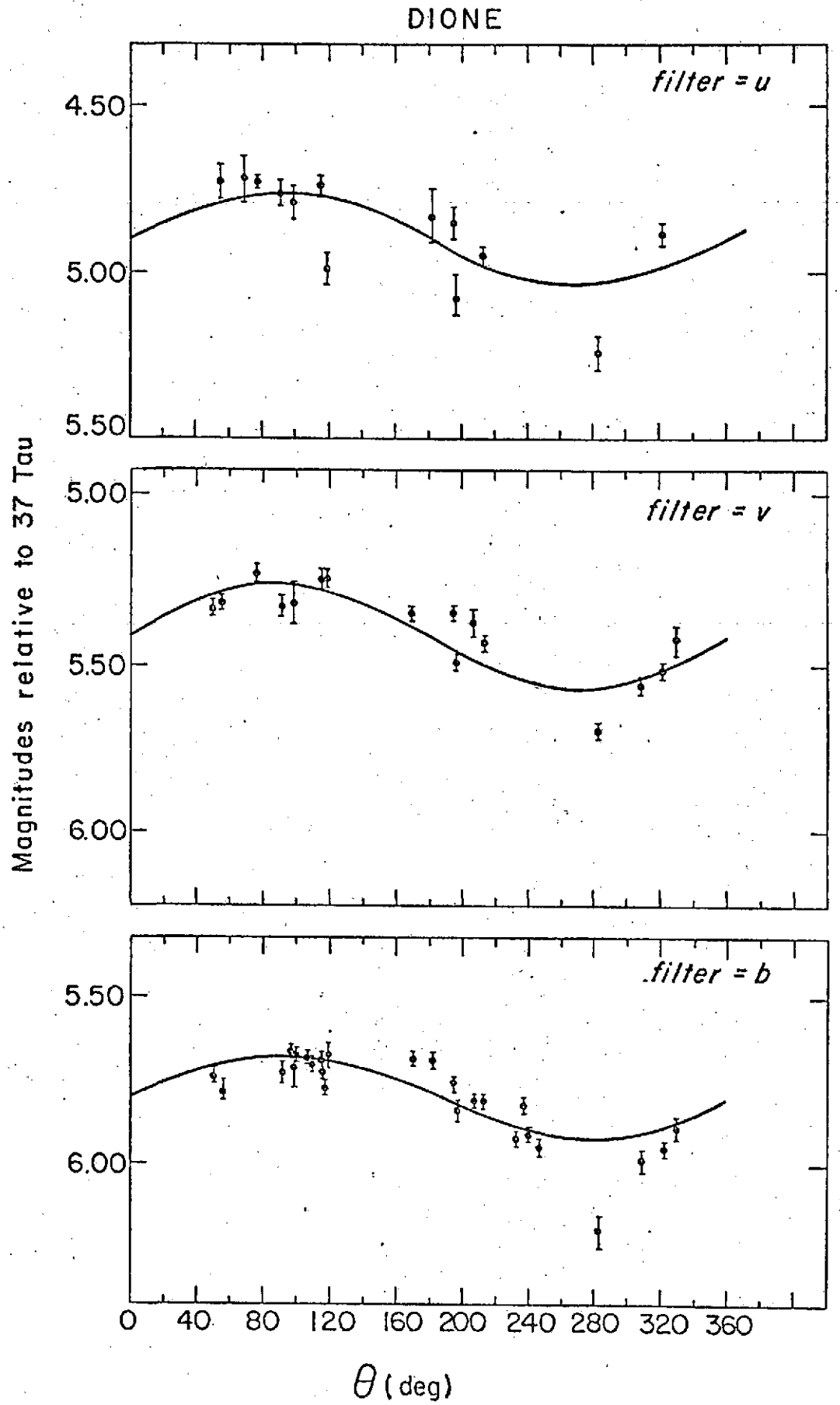
DIONE
filter = u
filter = v
filter = b
4.50
5.00
5.50
5.00
5.50
6.00
5.50
6.00
Magnitudes relative to 37 Tau
0
40
80
120
160
200
240
280
320
360
θ (deg)

Figure 5.

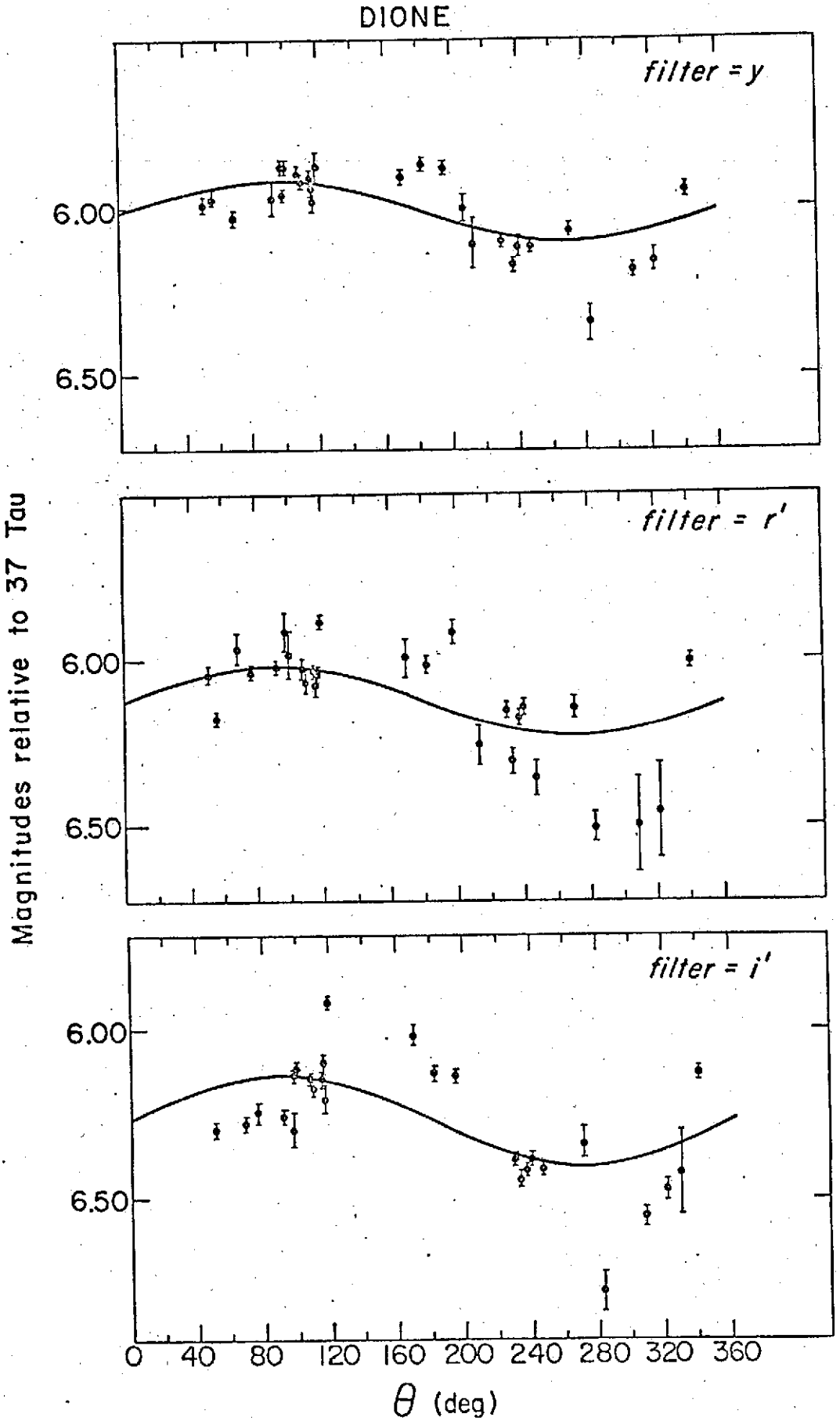
DIONE
filter = y
filter = r'
filter = i'
6.00
6.50
Magnitudes relative to 37 Tau
0
40
80
120
160
200
240
280
320
360
θ (deg)

Figure 5a.

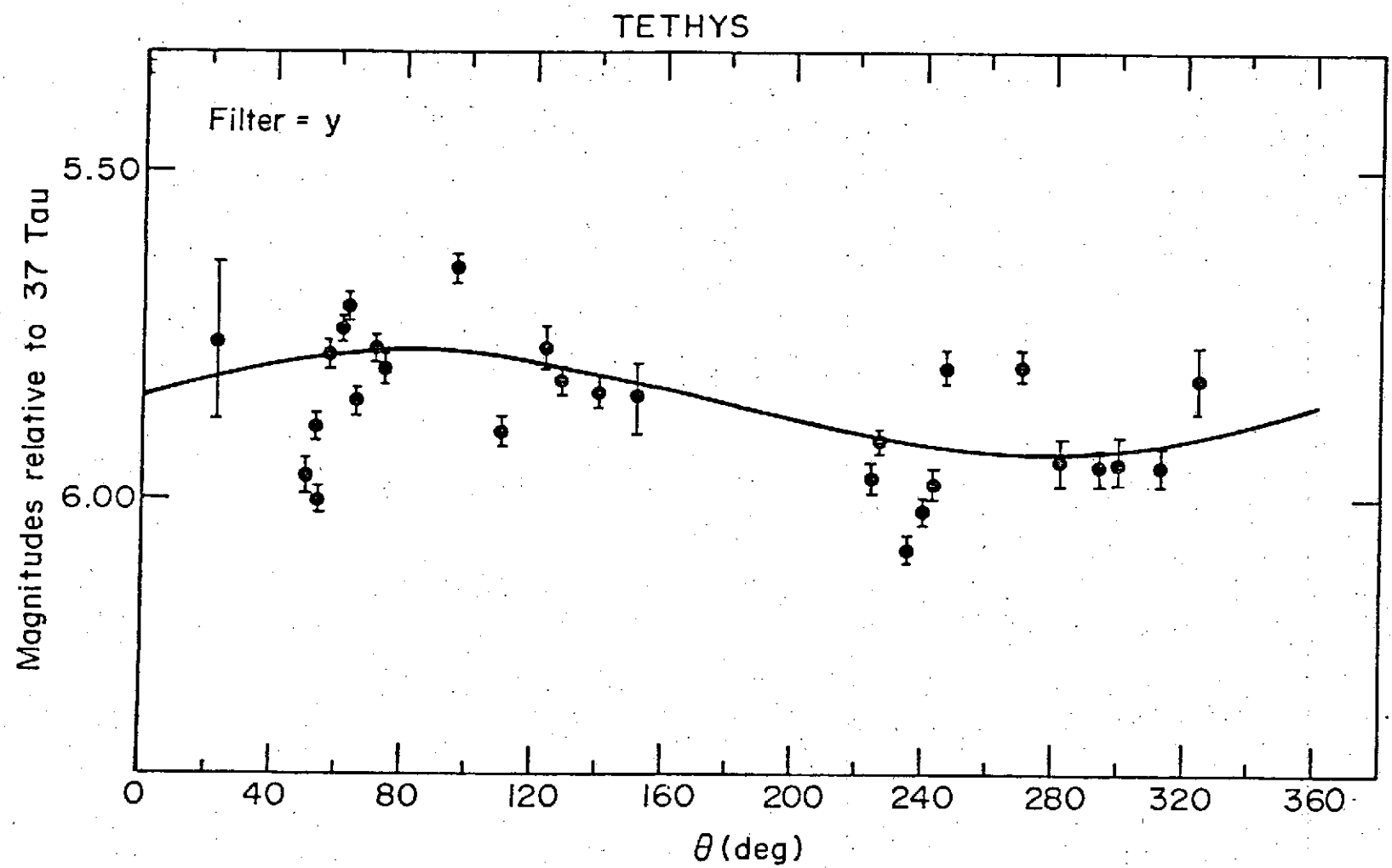
TETHYS
Filter = y
5.50
6.00
Magnitudes relative to 37 Tau
0
40
80
120
160
200
240
280
320
360
θ (deg)

Figure 6.

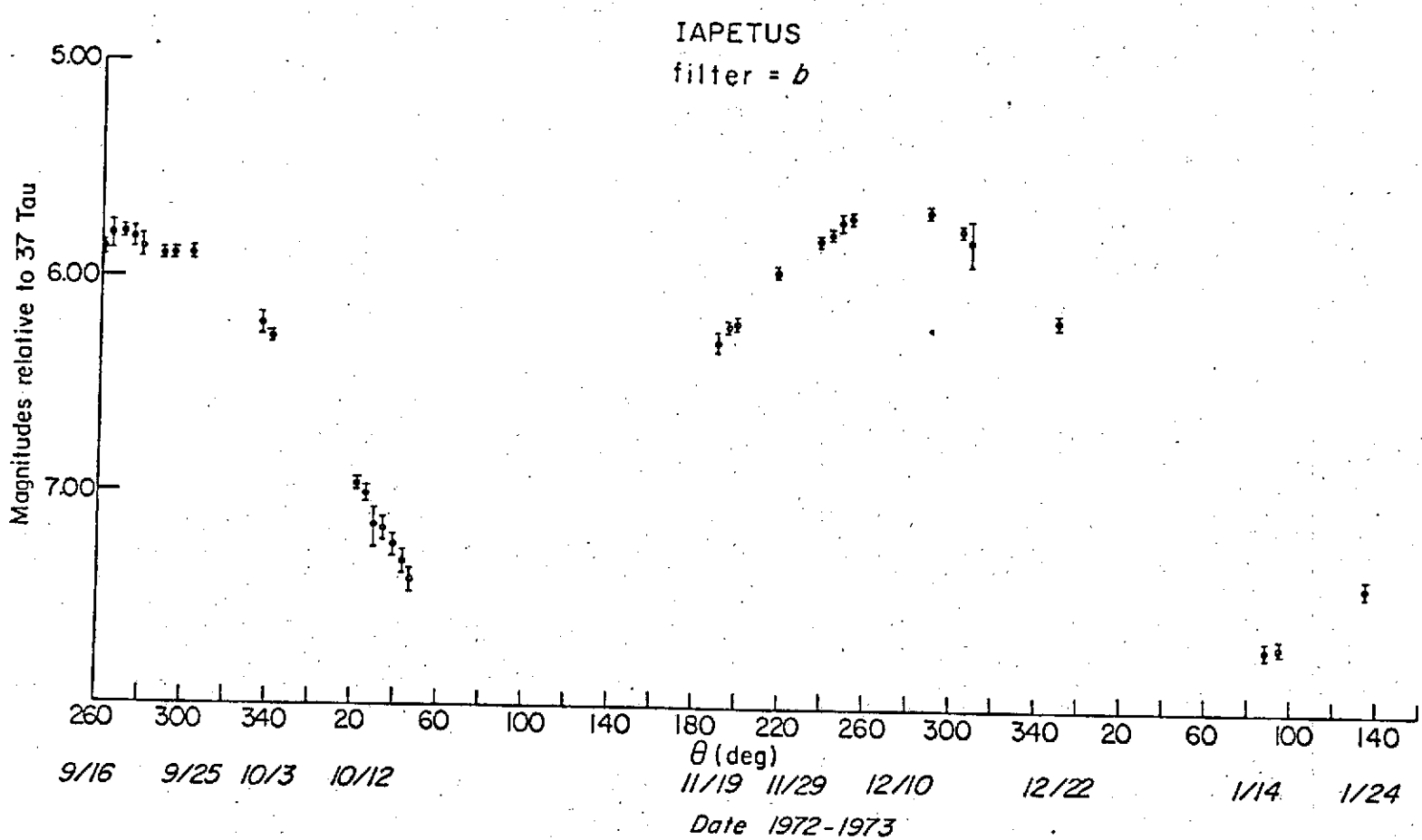
IAPETUS
filter = b
5.00
6.00
7.00
Magnitudes relative to 37 Tau
260
300
340
20
60
100
140
180
220
260
300
340
20
60
100
140
θ (deg)
9/16
9/25
10/3
10/12
11/19
11/29
12/10
12/22
1/14
1/24
Date 1972-1973

Figure 7.

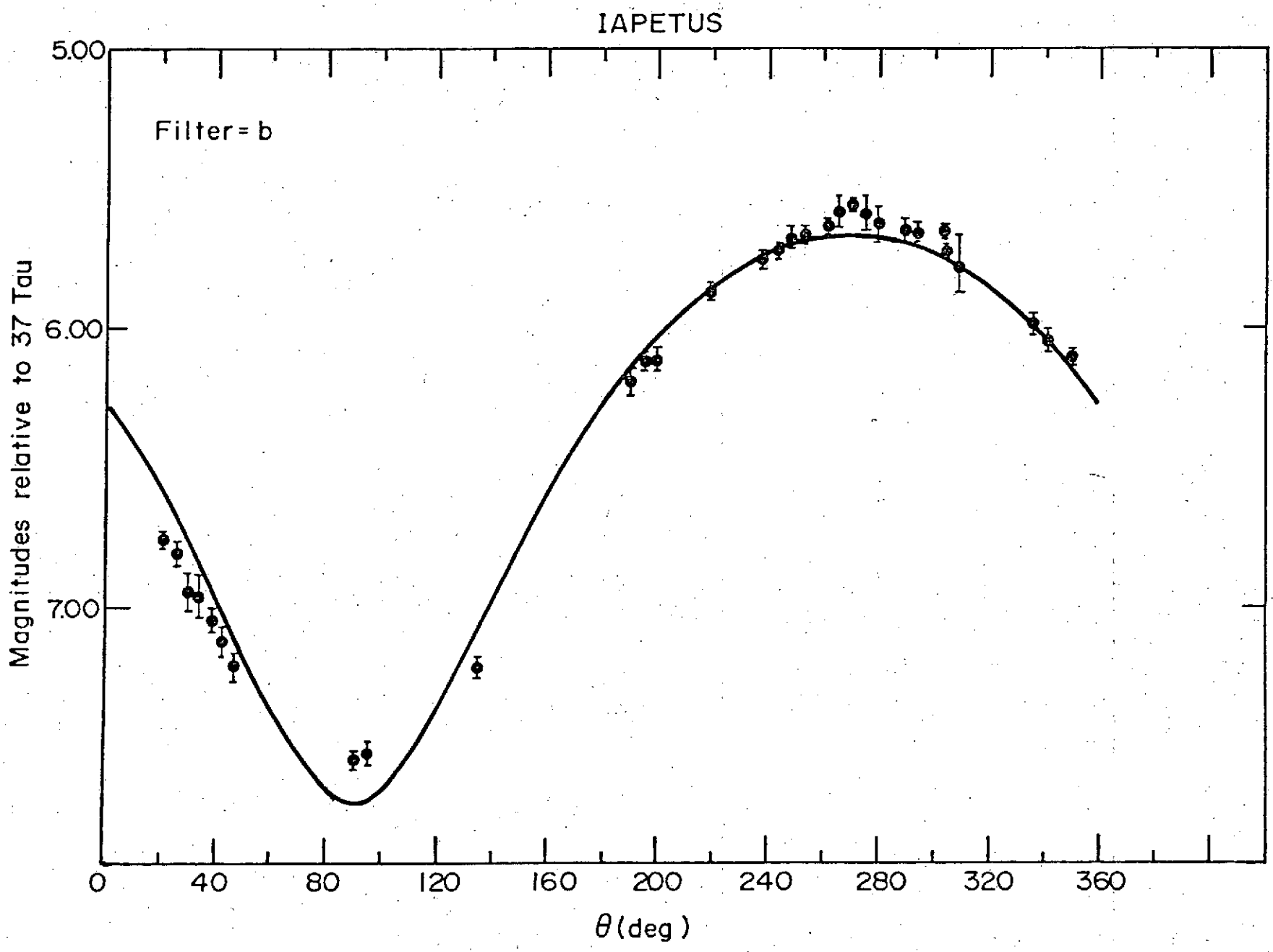
IAPETUS
Filter = b
5.00
6.00
7.00
Magnitudes relative to 37 Tau
0
40
80
120
160
200
240
280
320
360
θ (deg)

Figure 8.

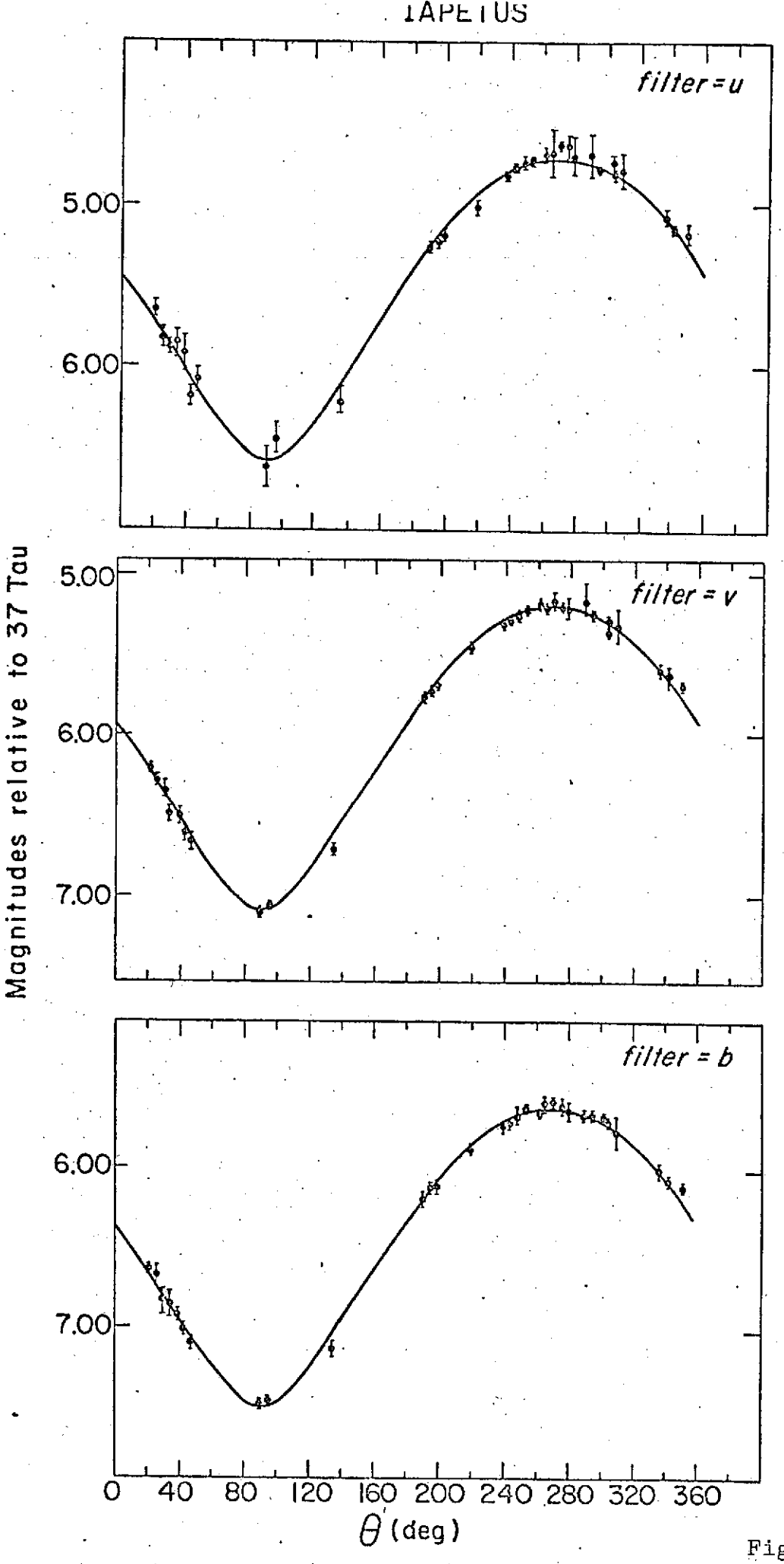
IAPETUS
filter = u
filter = v
filter = b
5.00
6.00
7.00
Magnitudes relative to 37 Tau
0
40
80
120
160
200
240
280
320
360
θ (deg)

Figure 9.

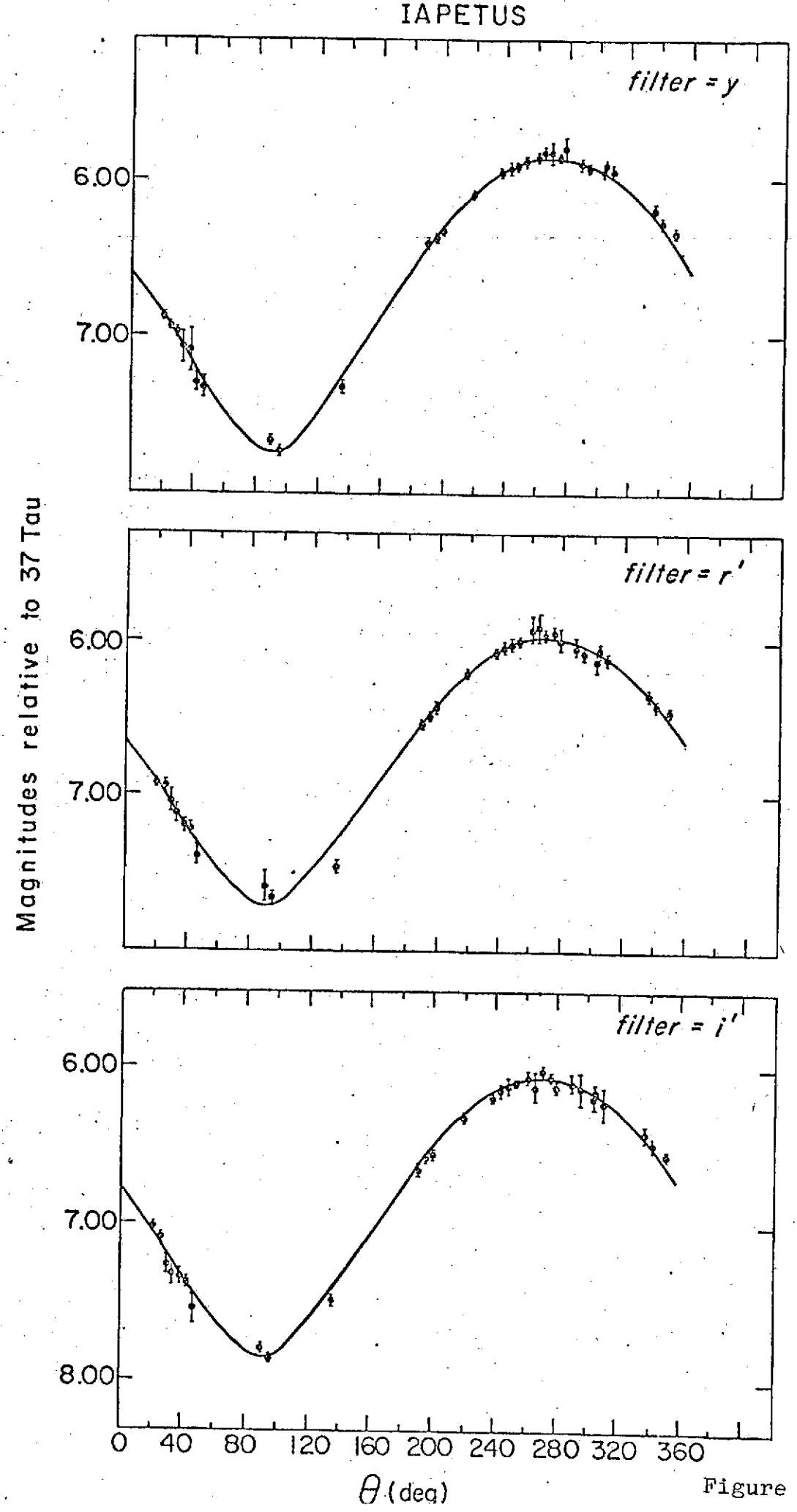
IAPETUS
filter = y
filter = r'
filter = i'
6.00
7.00
8.00
Magnitudes relative to 37 Tau
0
40
80
120
160
200
240
280
320
360
θ (deg)

Figure 9a.

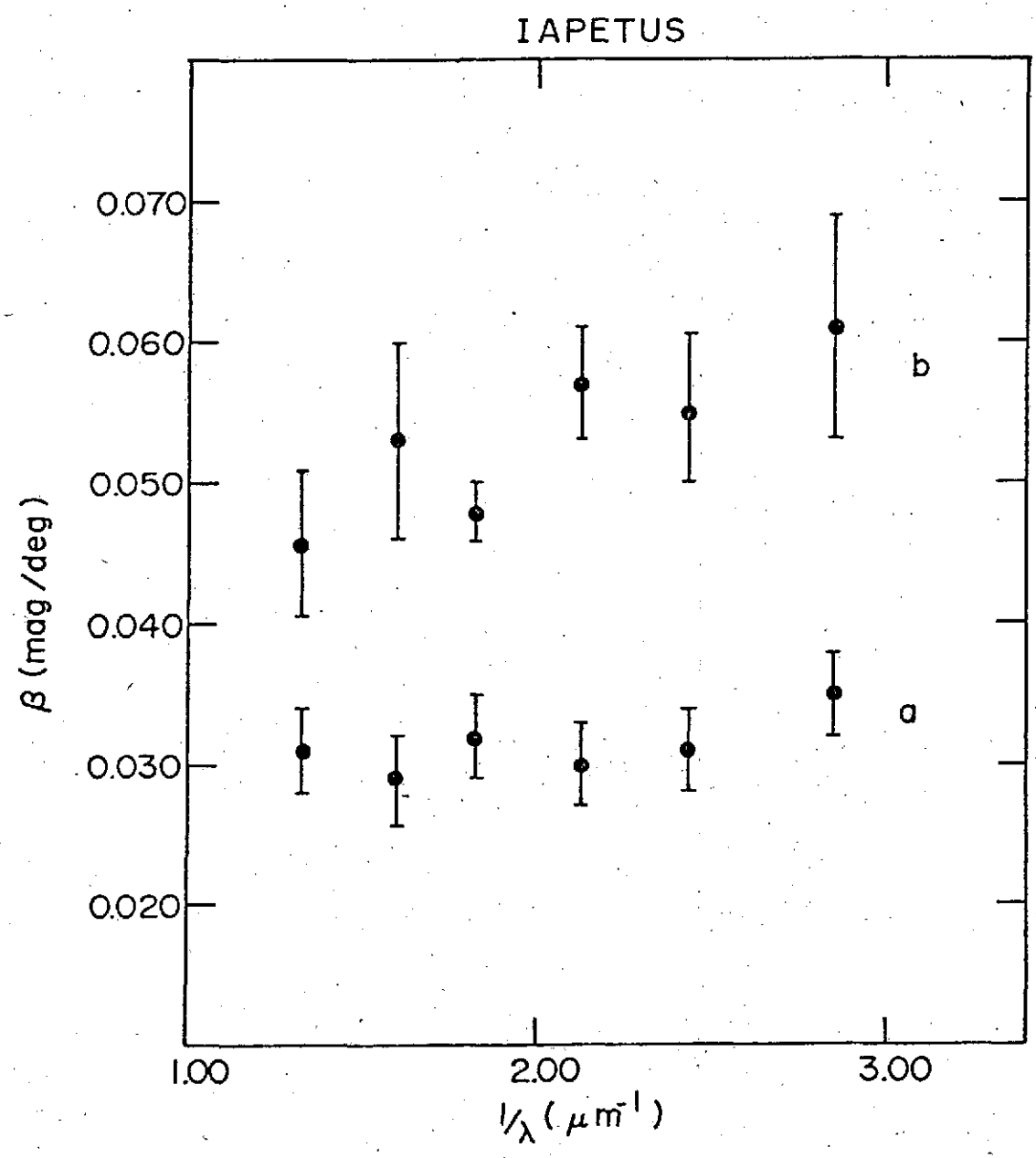
IAPETUS
0.070
0.060
0.050
0.040
0.030
0.020
β (mag/deg)
b
a
1.00
2.00
3.00
1/λ (μm⁻¹)

Figure 10.

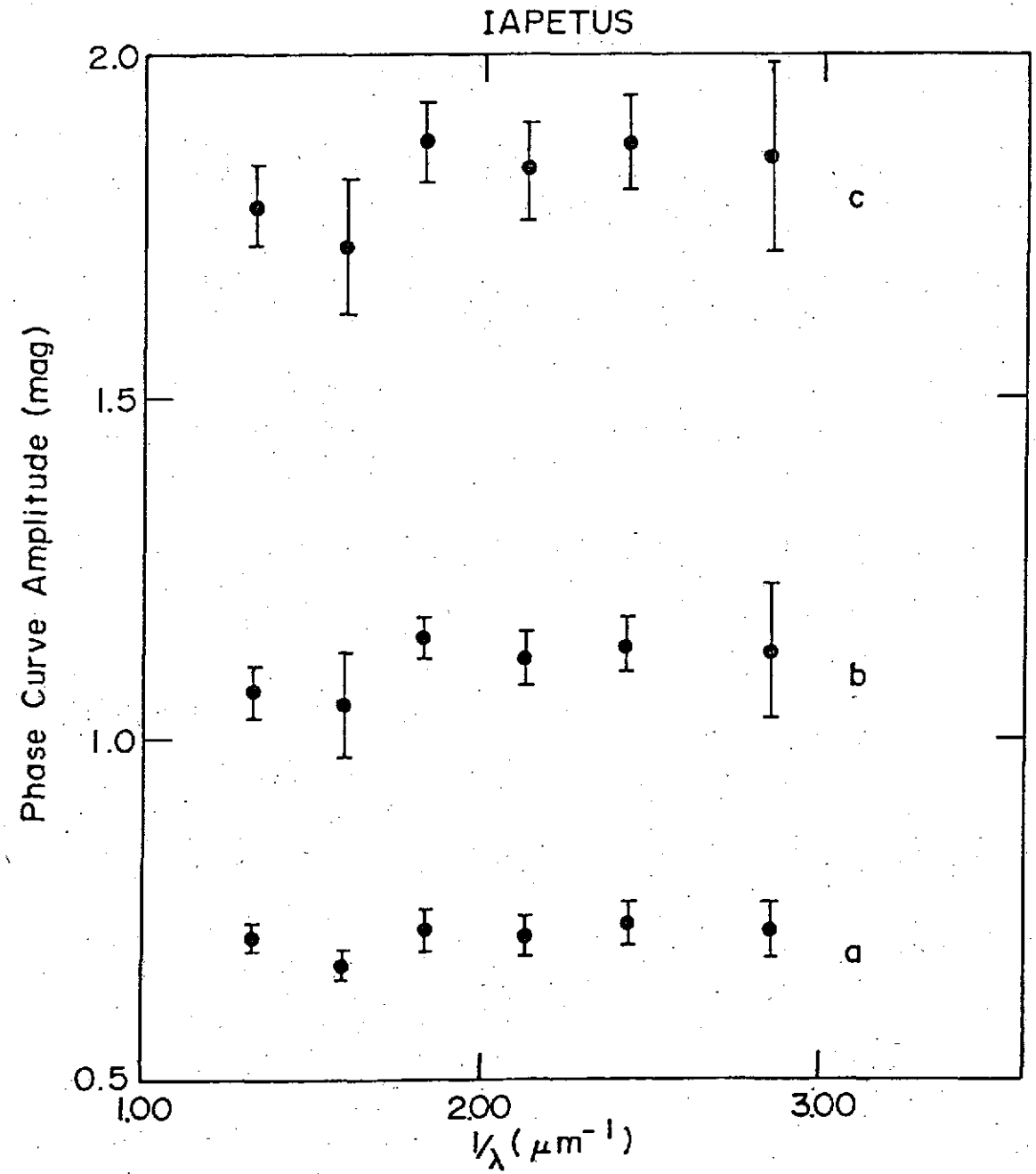
IAPETUS
2.0
1.5
1.0
0.5
Phase Curve Amplitude (mag)
c
b
a
1.00
2.00
3.00
1/λ (μm⁻¹)

Figure 11.

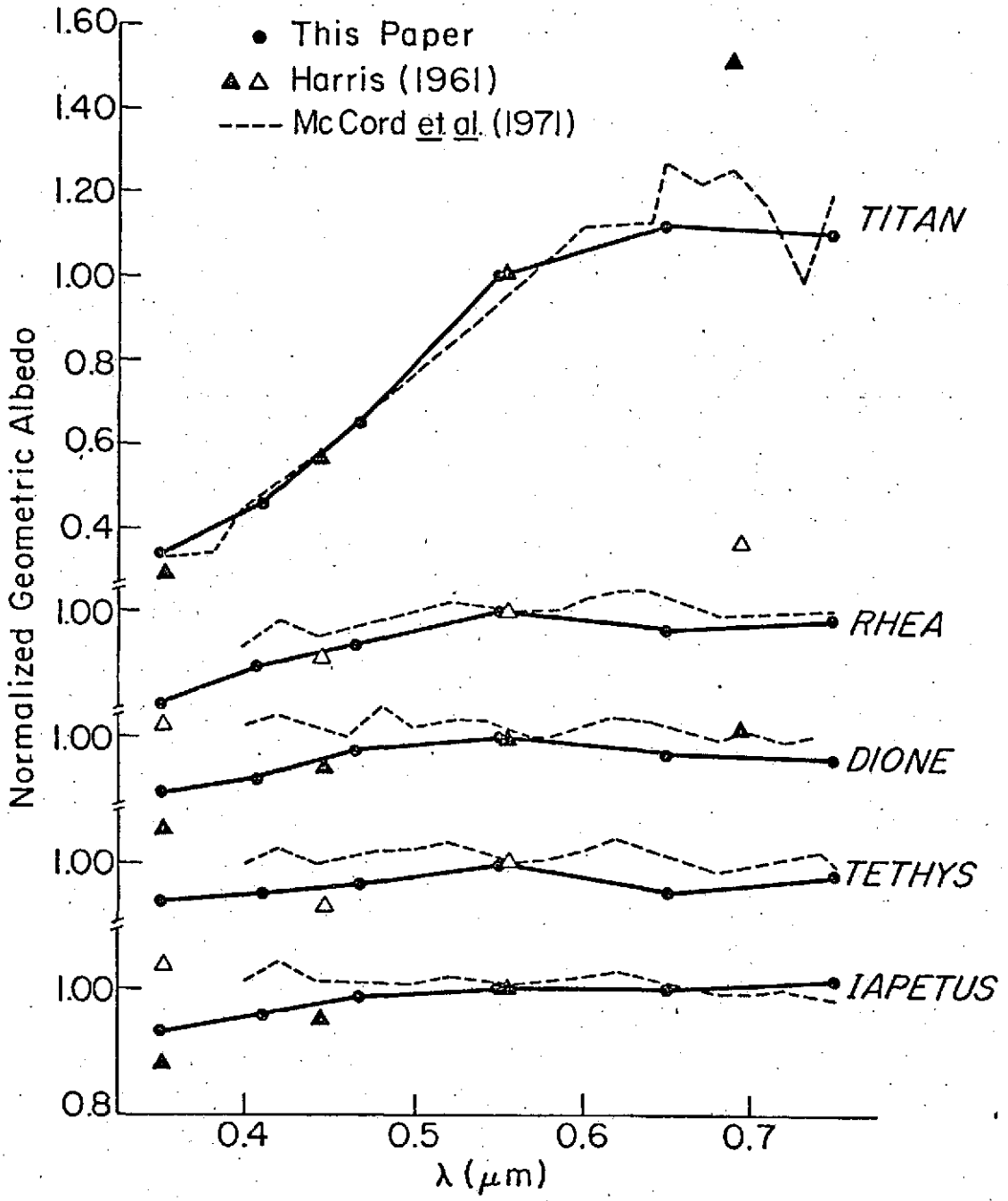
This Paper
Harris (1961)
McCord et al. (1971)
TITAN
RHEA
DIONE
TETHYS
IAPETUS
Normalized Geometric Albedo
λ (μm)
1.60
1.40
1.20
1.00
0.8
0.6
0.4
0.5
0.7

Figure 12.

Filter	u	v	b	y	r'	i'
λ (Å)	3500	4110	4670	5470	6239	~7500
Full-Width at Half-Maximum (Å)	300	190	180	230	256	~ 500
Nominal Extinction Coefficient (mag /airmass)	.47	.24	.15	.11	.09	.07

Table 1: Filter characteristics and extinction coefficients.

Table 2. Titan.

Date 1972-1973	Hours U.T.	Solar Phase α(deg)	Orbital Phase θ(deg)	Magnitudes Relative to 37 Tau at Mean Opposition					
				u	v	b	y	r'	i'
Sept. 15	13	6.4	348	3.96±.07		4.21±.03	3.96±.02	3.88±.03	4.09±.03
16	12	6.4	10	3.98±.04	4.16±.05	4.26±.04	3.99±.03	3.88±.05	4.08±.03
17	12	6.4	31	4.00±.07	4.14±.07	4.22±.03	3.98±.05	3.87±.04	4.08±.05
18	13	6.4	54	3.95±.04	4.11±.04	4 20±.03	3.95±.02	3.88±.02	4.02±.03
19	11	6.4	74	3.99±.04	4.13±.03	4.21±.01	3.95±.02	3.89±.01	4.03±.01
20	12	6.3	96	3.96±.07	4.13±.03	4.22±.02	3.97±.03	3.88±.03	4.06±.03
22	12	6.3	140		4.12±.03	4.23±.02	3.96±.02	3.90±.01	4.07±.04
23	15	6.3	166		4.21±.06	4.26±.04	3.99±.04	3.93±.02	4.08±.02
25	11	6.2	209	3.94±.04	4.11±.03	4.22±.03	3.98±.03	3.89±.04	4.06±.04
Oct. 2	13	6.0	12	4.03±.05	4.12±.02	4.20±.03	3.95±.03	3.88±.03	4.03±.03
3	12	6.0	32	3.95±.02	4.11±.03	4.19±.01	3.95±.02	3.88±.03	4.05±.02
12	13	5.6	212	3.95±.02	4.12±.02	4.21±.02	3.95±.02	3.91±.02	4.07±.02
13	12	5.5	258	3.97±.02	4.12±.02	4.17±.02	3.91±.02	3.85±.02	4.04±.02
14	10	5.5	280	3.95±.02	4.13±.02	4.21±.03	3.92±.03	3.91±.03	4.08±.03
15	12	5.4	304	3 96±.05	4.12±.01	4.21±.02	3.95±.02	3.89±.02	4.05±.01
16	11	5.4	326	3.95±.03	4.12±.03	4.21±.02	3.95±.02	3.88±.02	4.03±.02
17	11	5.3	349	3.97±.02	4.13±.02	4.22±.02	3.95±.02	3.90±.03	4.06±.03
18	10	5.2	11	3.96±.05	4.16±.02	4.23±.02	3.96±.02	3.89±.03	4.05±.01

Table 2. (continued) Titan.

Date 1972-1973	Hours U.T.	Solar Phase α(deg)	Orbital Phase θ(deg)	Magnitudes Relative to 37 Tau at Mean Opposition					
				u	v	b	y	r'	i'
Nov. 1	9	4.1	327	3.92±.02	4.10±.02	4.19±.02	3.93±.02	3.88±.02	4.03±.02
19	9	2.4	14	3.92±.04		4.18±.02	3.94±.01	3.88±.01	4.04±.01
20	8	2.2	35	3.94±.03	4.12±.02	4.22±.03	3.96±.03	3.93±.03	4.08±.03
21	10	2.1	58	3.93±.03	4.10±.02	4.19±.01	3.94±.01	3.89±.01	4.04±.01
25	21	1.7	157	3.91±.02	4.08±.02	4.17±.02	3.92±.01	3.87±.02	4.03±.01
29	9	1.2	239	3.89±.03	4.08±.02	4.19±.02	3.93±.01	3.88±.01	4.05±.02
30	9	1.1	263	3.90±.03	4.11±.04	4.18±.03	3.94±.02	3.89±.02	4.05±.02
Dec. 1	8	1.0	284	3.90±.02	4.08±.01	4.17±.02	3.93±.02	3.88±.02	4.04±.02
2	8	0.9	307	3.90±.02	4.08±.01	4.18±.01	3.93±.01	3.88±.01	4.05±.01
13	11	0.5	196	3.89±.02	4.08±.01	4.18±.01	3.93±.02	3.87±.03	4.05±.03
14	6	0.6	215	3.86±.02	4.04±.02	4.16±.02	3.93±.02	3.90±.02	4.04±.02
Jan. 16	6	4.1	243	3.91±.03	4.08±.04	4.18±.03	3.92±.04	3.87±.05	4.05±.04

Table 3.

Date 1972-1973	Hours U. T.	Solar Phase α(deg)	Orbital Phase θ(deg)	Rhea (7" Aperture) Magnitudes Relative to 37 Tau at Mean Opposition					
				u	v	b	y	r'	i'
Sept. 19	12.5	6.4	147	4.43±.03	4.83±.01	5.21±.01	5.35±.01	5.44±.02	5.56±.02
22	12.9	6.3	27	4.49±.04	4.88±.05	5.26±.05	5.42±.02	5.53±.01	5.65±.02
25	12.2	6.2	265	4.66±.08	5.06±.03	5.42±.03	5.55±.05	5.67±.03	5.77±.05
Oct. 12	15.1	5.6	189	4.54±.02	4.88±.02	5.27±.01	5.47±.03	5.49±.03	5.71±.04
13	12.9	5.5	261	4.65±.02	5.05±.05	5.55±.07	5.63±.05	5.61±.07	5.87±.03
14	11.9	5.5	337	4.66±.05	4.95±.03	5.37±.04	5.48±.02	5.52±.03	5.70±.02
15	14.6	5.4	66	4.39±.02	4.77±.05	5.21±.03	5.35±.04	5.44±.03	
15	12.2	5.4	58	4.38±.02	4.80±.04	5.20±.01	5.37±.03	5.47±.02	5.57±.02
16	13.5	5.4	142	4.40±.01	4.84±.02	5.21±.01	5.35±.02	5.45±.02	5.61±.10
16	10.9	5.4	134		4.81±.05	5.21±.04	5.38±.02	5.47±.02	5.66±.10
17	10.4	5.3	210	4.59±.08	4.96±.02	5.35±.03	5.52±.02	5.55±.05	5.67±.01
17	12.8	5.3	219	4.57±.01	4.95±.02	5.37±.06		5.60±.02	
17	14.2	5.3	224	4.56±.05		5.37±.02	5.52±.01		
18	10.0	5.2	290	4.59±.02	5.04±.03	5.40±.03		5.61±.05	5.72±.02
18	12.3	5.2	297				5.52±.02	5.69±.03	5.92±.04
18	13.7	5.2	302		4.95±.05	5.38±.03	5.50±.03	5.70±.02	5.77±.02

Table 3. (continued)

Date 1972-1973	Hours U.T.	Solar Phase α(deg)	Orbital Phase θ(deg)	Rhea (7" Aperture) Magnitudes Relative to 37 Tau at Mean Opposition					
				u	v	b	y	r'	i'
Nov. 19	11.4 h	2.4	327	4.45±.06	4.91±.06	5.26±.02	5.40±.01	5.48±.03	5.62±.02
20	10.4	2.2	43	4.30±.01	4.73±.05	5.22±.06	5.31±.03	5.41±.04	5.53±.04
25	8.9	1.7	77		4.66±.01	5.15±.02	5.22±.01	5.32±.01	5.50±.02
25	13.0	1.7	90		4.73±.03	5.06±.01	5.24±.02	5.32±.02	5.45±.01
30	11.2	1.1	124			5.04±.02	5.23±.02	5.35±.04	5.46±.02
Dec. 1	8.3	1.0	194			5.30±.02	5.35±.01	5.45±.01	5.63±.01
1	10.1	1.0	200			5.20±.01	5.36±.01	5.45±.02	5.57±.01
1	11.4	1.0	204			5.22±.01	5.36±.01	5.53±.01	5.57±.02
2	10.3	0.9	280			5.22±.01	5.43±.05	5.59±.05	5.63±.02
2	11.5	0.9	284	4.44±.02		5.22±.01	5.37±.01	5.47±.01	5.60±.02
10	11.6	0.3	203					5.44±.03	
13	10.0	0.5	76			5.04±.01	5.22±.02	5.29±.02	5.40±.02
13	13.8	0.5	89				5.21±.02	5.33±.02	5.38±.02
14	7.2	0.6	148	4.25±.02	4.72±.02	5.12±.03	5.24±.02	5.35±.02	5.47±.02

Table 3. (continued)

Date 1972-1973	Hours U.T.	Solar Phase α(deg)	Orbital Phase θ(deg)	Rhea (15" Aperture) Magnitudes Relative to 37 Tau at Mean Opposition					
				u	v	b	y	r'	i'
Oct. 2	11.0	6.0	98	4.39±.02	4.81±.02	5.24±.02	5.29±.02	5.40±.02	5.45±.03
2	12.7	6.0	104	4.43±.02	4.85±.02	5.27±.02	5.39±.03	5.51±.05	5.62±.03
2	14.2	6.0	109	4.37±.09	4.79±.04	5.21±.02	5.37±.03	5.47±.02	5.58±.02
Nov. 21	9.5	2.1	120	4.34±.02	4.76±.02	5.15±.02	5.30±.02	5.40±.03	5.50±.02
21	12.1	2.1	129	4.27±.02	4.75±.02	5.14±.02	5.29±.02	5.40±.02	5.49±.02
25	10.7	1.7	83	4.23±.02	4.63±.02	5.01±.02	5.16±.02	5.24±.02	5.33±.02
25	13.9	1.7	94	4.25±.02	4.67±.02	5.06±.02	5.21±.02	5.31±.02	5.42±.02
29	7.7	1.2	32	4.35±.02	4.79±.02	5.14±.02	5.31±.02	5.44±.02	5.54±.02
29	9.4	1.2	37	4.29±.02	4.72±.02	5.12±.02	5.32±.02	5.44±.02	5.55±.02
29	11.4	1.2	44	4.31±.02	4.74±.02	5.14±.02	5.32±.02	5.39±.02	5.55±.02
30	7.8	1.1	113	4.15±.07	4.67±.02	5.07±.02	5.24±.02	5.34±.02	5.45±.02
30	8.2	1.1	114	4.21±.02	4.66±.02	5.08±.02	5.23±.02	5.38±.02	5.44±.02
30	9.8	1.1	119	4.21±.02	4.68±.02	5.06±.02	5.24±.02	5.33±.02	5.43±.02
Dec. 2	7.1	0.9	270	4.40±.02	4.79±.02	5.18±.02	5.35±.02	5.44±.02	5.55±.02
2	8.0	0.9	273	4.47±.02	4.85±.02	5.26±.02	5.42±.02	5.53±.02	5.65±.02
Jan. 14	8.1	4.0	103	4.35±.02	4.78±.02	5.20±.02	5.36±.02	5.47±.02	5.61±.02
16	6.1	4.1	256	4.54±.02	4.93±.02	5.30±.02	5.44±.02	5.52±.02	5.62±.02

Table 4. Dione.

Date 1972-1973	Hours U.T.	Solar Phase α(deg)	Orbital Phase θ(deg)	Magnitudes Relative to 37 Tau at Mean Opposition					
				u	v	b	y	r'	i'
Sept. 15	13.5	6.4	207		5.50±.04	5.91±.02	6.06±.04		
Oct. 13	14.5	5.5	170		5.45±.02	5.76±.02	5.96±.02	6.01±.06	5.93±.03
14	12.3	5.5	283	5.40±.04	5.81±.02	6.28±.04	6.39±.05	6.52±.04	6.69±.06
15	12.5	5.4	56	4.89±.05	5.42±.02	5.86±.02	6.02±.02	6.19±.02	
15	14.9	5.4	69	4.88±.08			6.08±.02	5.98±.05	6.20±.02
16	11.4	5.4	182	4.99±.08		5.77±.02	5.92±.02	6.03±.02	6.05±.02
16	13.8	5.4	195	5.01±.05	5.45±.02	5.85±.02	5.93±.02	5.93±.04	6.06±.04
17	10.7	5.3	309		5.66±.02	6.07±.03	6.24±.02	6.51±.14	6.48±.03
17	13.1	5.3	322	5.04±.03	5.62±.02	6.03±.02	6.21±.03	6.47±.14	6.40±.03
17	14.5	5.3	330		5.53±.04	5.97±.03			6.35±.13
18	10.3	5.2	77	4.88±.02	5.33±.02			6.05±.02	6.17±.03
18	12.6	5.2	92	4.91±.04	5.43±.03	5.81±.03	6.02±.05	6.04±.02	6.18±.02
18	14.0	5.2	99	4.94±.04	5.42±.06	5.79±.06	6.01±.02		6.22±.05
Nov. 1	9.4	4.1	116	4.86±.03	5.32±.03	5.78±.02	5.98±.02	6.08±.03	6.04±.02
1	9.9	4.1	119	5.11±.04	5.32±.03	5.73±.04	5.92±.04	5.89±.02	5.86±.02
25	12.3	1.7	51		5.36±.02	5.76±.02	6.01±.02	6.05±.02	6.27±.02
29	8.6	1.2	197	5.11±.06	5.51±.02	5.85±.03			
29	11.6	1.2	213	4.98±.02	5.45±.02	5.82±.02	6.12±.07	6.29±.06	
30	10.6	1.1	339						

Table 4. (continued) Dione.

Date 1972-1973	Hours U.T.	Solar Phase α(deg)	Orbital Phase θ(deg)	Magnitudes Relative to 37 Tau at Mean Opposition					
				u	v	b	y	r'	i'
30	10.9	1.1	341				5.96±.02	6.00±.02	6.11±.02
Dec. 1	8.2	1.0	98			5.67±.02	5.89±.02	5.91±.06	6.12±.02
1	8.5	1.0	100			5.68±.06	5.89±.02	5.98±.07	6.10±.02
1	9.9	1.0	108			5.69±.02	5.91±.02	6.02±.03	6.13±.02
1	10.3	1.0	110			5.71±.02	5.93±.02	6.06±.03	6.16±.02
1	11.2	1.0	115			5.70±.02	5.92±.02	6.03±.02	6.13±.03
1	11.7	1.0	117			5.78±.02	5.99±.03	6.04±.02	6.19±.04
2	8.2	0.9	230				6.11±.02	6.25±.02	6.38±.02
2	9.6	0.9	237			5.83±.02	6.18±.02	6.27±.02	6.41±.02
2	10.0	0.9	240			5.92±.02	6.13±.03	6.24±.02	6.38±.02
2	11.3	0.9	247			5.96±.02	6.13±.02	6.35±.05	6.41±.02
13	7.3	0.5	233			5.93±.02		6.30±.04	6.44±.02
13	14.3	0.5	271				6.07±.02	6.14±.03	6.33±.05

Table 5. Tethys.

Date 1972–1973	Hours U.T.	Solar Phase α(deg)	Orbital Phase θ(deg)	Magnitudes Relative to 37 Tau at Mean Opposition					
				u	v	b	y	r'	i'
Oct. 13	13.3	5.5	270	5.14±.03	5.38±.03	5.73±.02	5.90±.02	5.95±.03	6.01±.04
14	12.7	5.5	96	4.72±.03		5.61±.02	5.75±02	5.77±.05	5.92±.03
15	12.9	5.4	282	4.95±.03	5.43±.02	5.84±.02	6.05±.03	6.22±.02	6.35±.03
15	15.1	5.4	300		5.35±.05	5.76±.04	6.05±.03	6.08±.02	6.22±.06
16	11.8	5.4	110	4.87±.03	5.32±.02	5.77±.02	6.00±.02	6.12±.02	6.21±.02
16	14.1	5.4	128	4.90±.09	5.28±.02	5.74±.02	5.92±.02	6.04±.05	6.29±.11
17	11.0	5.3	294	4.93±.03	5.47±.02	5.87±.02	6.05±.02	6.22±.04	6.30±.02
17	13.4	5.3	313	4.92±.04	5.36±.03		6.05±.02	6.22±.05	6.20±.02
17	14.8	5.3	324	4.88±.09	5.50±.08	5.73±.02	5.91±.05	6.13±.13	6.28±.02
18	10.6	5.2	122	4.79±.02	5.28±.02	5.69±.02	5.87±.02	6.08±.09	6.25±.05
18	12.9	5.2	140	4.82±.02	5.27±.04	5.73±.02	5.94±.02	5.98±.04	6.18±.03
18	14.3	5.2	151		5.29±.06		5.95±.05	6.15±.07	6.09±.08
Nov. 29	11.8	1.2	224	4.84±.02	5.32±.02	5.72±.02	5.99±.02	6.04±.02	6.19±.05
29	12.0	1.2	226	4.79±.05	5.28±.02	5.65±.02	5.93±.02	5.98±.03	6.32±.10
30	11.1	1.1	50			5.68±.02	5.99±.02	6.27±.04	6.32±.11
30	11.5	1.1	53				5.90±.02	6.07±.03	
30	11.7	1.1	54				6.02±.02	6.16±.06	
30	12.0	1.1	56				5.80±.02	5.97±.09	

Table 5. (continued) Tethys.

Date 1972-1973	Hours U.T.	Solar Phase α(deg)	Orbital Phase θ(deg)	Magnitudes Relative to 37 Tau at Mean Opposition					
				u	v	b	y	r'	i'
Dec. 1	10.5	1.0	235			6.12±.02	6.10±.02	6.31±.02	6.50±.02
1	11.1	1.0	240			5.88±.05	6.04±.02	6.28±.03	6.50±.06
1	11.5	1.0	243			5.76±.02	6.00±.02	6.10±.02	6.38±.04
1	11.8	1.0	246			5.64±.02	5.82±.02	5.92±.02	5.98±.02
2	9.8	0.9	61			5.55±.02	5.76±.02	5.85±.02	5.99±.03
2	10.1	0.9	63			5.57±.02	5.73±.02	5.88±.02	5.95±.02
2	10.4	0.9	65			5.66±.02	5.87±.02	6.06±.03	6.23±.03
2	11.1	0.9	71			5.58±.02	5.79±.02	5.89±.02	6.03±.02
2	11.5	0.9	74			5.60±.02	5.82±.02	5.86±.02	6.06±.02
13	12.6	0.5	22			6.04±.05	5.77±.12	6.34±.17	5.73±.02

Table 6. Iapetus.

Date 1972-1973	Hours U.T.	Solar Phase α(deg)	Orbital Phase θ(deg)	Magnitudes Relative to 37 Tau at Mean Opposition					
				u	v	b	y	r'	i'
Sept. 16	12	6.4	261	4.91±.04	5.39±.03	5.87±.02	6.06±.02	6.11±.08	6.26±.04
17	12	6.4	265	4.90±.14	5.41±.03	5.81±.06	6.03±.03	6.10±.09	6.33±.09
18	14	6.4	270	4.85±.03	5.37±.05	5.80±.02	6.03±.06	6.15±.03	6.23±.03
19	12	6.4	275	4.85±.07	5.40±.02	5.82±.05	6.06±.02	6.14±.04	6.26±.02
20	12	6.3	279	4.92±.12	5.40±.06	5.86±.05	6.01± 07	6.18±.07	6.32±.03
22	12	6.3	289	4.90±.14	5.36±.10	5.89±.02	6.11±.03	6.23±.05	6.30±.05
23	13	6.3	294	4.00±.01	5.45±.01	5.89±.02	6.13±.01	6.26±.05	6.32±.10
25	11	6.2	303	4.96±.04	5.55±.03	5.89±.04	6.13±.04	6.30±.07	6.38±.07
Oct. 2	13	6.0	336	5.28±.04	5.78±.04	6.21±.03	6.39±.04	6.52±.03	6.59±.05
3	13	6.0	341	5.35±.03	5.81±.04	6.27±.02	6.47±.03	6.59±.03	6.67±.04
12	13	5.6	21	5.99±.05	6.51±.02	6.96±.02	7.16±.01	7.22±.02	7.29±.02
13	12	5.5	26	6.17±.06	6.58±.04	7.00±.03	7.21±.01	7.23±.04	7.34±.03
14	11	5.5	30	6.22±.05	6.63±.04	7.15±.10	7.24±.03	7.33±.07	7.52±.06
15	12	5.4	34	6.19±.08	6.79±.04	7.17±.06	7.34±.10	7.41±.06	7.58±.07
16	12	5.4	39	6.25±.11	6.80±.05	7.24±.05	7.36±.14	7.49±.04	7.60±.05
17	11	5.3	43	6.51±.06	6.90±.05	7.32±.05	7.56±.05	7.50±.04	7.62±.04
18	10	5.2	47	6.40±.08	6.95±.05	7.40±.05	7.58±.06	7.67±.05	7.79±.09
Nov. 19	10	2.4	190	5.34±.03	5.83±.03	6.28±.04	6.49±.03	6.60±.02	6.73±.03
20	9	2.2	195	5.30±.04	5.79±.01	6.21±.01	6.45±.01	6.54±.02	6.66±.02
21	11	2.1	199	5.26±.04	5.74±.03	6.19±.03	6.40±.02	6.49±.03	6.62±.04
25	13	1.7	219	5.07±.04	5.50±.02	5.95±.01	6.15±.02	6.26±.02	6.37±.03
29	9	1.2	238	4.86±.01	5.35±.02	5.80±.02	6.00±.01	6.11±.02	6.23±.02
30	8	1.1	243	4.81±.03	5.32±.02	5.77±.02	5.97±.04	6.08±.03	6.18±.03

Table 6. (continued) Iapetus.

Date 1972-1973	Hours U.T.	Solar Phase α(deg)	Orbital Phase θ(deg)	Magnitudes Relative to 37 Tau at Mean Opposition					
				u	v	b	y	r'	i'
Dec. 1	8	1.0	248	4.77±.04	5.29±.02	5.72±.03	5.95±.02	6.05±.04	6.15±.05
2	9	0.9	253	4.75±.03	5.24±.03	5.70±.02	5.91±.02	6.03±.02	6.13±.01
10	11	0.3	289	4.70±.02	5.20±.02	5.67±.02	5.90±.02	6.04±.02	6.07±.02
13	12	0.5	304	4.82±.03	5.31±.03	5.75±.01	5.94±.02	6.06±.04	6.16±.02
14	7	0.6	309	4.81±.10	5.34±.10	5.81±.10	5.97±.04	6.14±.04	6.24±.10
22	11	1.5	350	5.23±.06	5.74±.02	6.17±.02	6.39±.02	6.49±.02	6.61±.02
Jan. 14	7	4.0	90	6.85±.12	7.31±.03	7.70±.03	7.86±.03	7.80±.10	7.98±.03
15	7	4.0	95	6.68±.09	7.27±.02	7.68±.03	7.93±.02	7.87±.04	8.04±.03
24	7	4.8	135	6.50±.07	6.97±.03	7.40±.03	7.57±.04	7.71±.04	7.71±.03

	u	v	b	y	r'	i'
Table 7						
Titan						
β(mag/deg)	.014±.001	.010±.001	.006±.001	.005±.001	.002±.001	.001±.001
M_o (mag)	3.88±.01	4.07±.01	4.17±.01	3.93±.01	3.88±.01	4.04±.01
Table 8						
Rhea						
β(mag/deg)	.037±.003	.031±.003	.027±.003	.025±.002	.025±.003	.024±.004
$2\mu_o$(mag)	.24±.02	.20±.02	.18±.02	.19±.02	.19±.02	.20±.02
M_o (mag)	4.30±.01	4.73±.01	5.13±.01	5.29±.01	5.40±.01	5.52±.01
θ_o (deg)	7±5	12±8	0±7	0±5	-1±7	3±9
Table 9						
Dione						
β(1)	.045±.029	.016±.010	.012±.005	.009±.007	.003±.011	-.015±.011
β(2)	.029±.018	.021±.010	.015±.006	.009±.007	.003±.010	-.015±.012
$2\mu_o$(1)	$.32^{+.30}_{-.12}$	.36±.08	.30±.08	.24±.12	$.24^{+.10}_{-.06}$	$.32^{+.18}_{-.08}$
$2\mu_o$(2)	.23±.08	.33±.06	.23±.04	.19±.04	.23±.06	.27±.06
M_o(1)	4.82±.13	5.43±.05	5.83±.02	6.02±.02	6.12±.03	6.29±.04
M_o(2)	4.90±.07	5.41±.05	5.80±.02	6.01±.03	6.12±.03	6.27±.04

Table 9 (cont'd)	u	v	b	y	r'	i'
θ_o (1)	-21±32	16±10	34±19	32±15	10±22	29±18
θ_o (2)	0	0	0	0	0	0
Table 10						
Tethys						
β (1)	.066±.015	.009±.014	.014±.011	.019±.007	.011±.012	.016±.014
β (2)	.035±.012	.021±.008	.015±.010	.019±.007	.009±.012	.016±.014
$2\ \mu_o$ (1)	$.40^{+.20}_{-.12}$	$.11^{+.07}_{-.15}$	$.12^{+.20}_{-.07}$	.16±.06	$.19^{+.30}_{-.10}$	$.21^{+.48}_{-.09}$
$2\ \mu_o$ (2)	.20±.05	.12±.03	.12±.05	.16±.04	.15±.06	.16±.07
M_o (1)	4.52±.08	5.29±.08	5.66±.04	5.85±.03	6.00±.04	6.09±.05
M_o (2)	4.69±.06	5.22±.04	5.66±.04	5.85±.03	6.00±.04	6.09±.05
θ_o (1)	-35±15	54±70	-7±50	-1±25	33±30	-41±30
θ_o (2)	0	0	0	0	0	0

Table 7. Titan: derived light-curve parameters.

Table 8. Rhea: derived light-curve parameters.

Table 9. Dione: derived light-curve parameters. Two solutions are given. See text for details.

Table 10. Tethys: derived light-curve parameters. Two solutions are given. See text for details.

	u	v	b	y	r'	i'
M_o(mag)	5.44±.04	5.94±.02	6.37±.02	6.59±.02	6.66±.02	6.78±.03
β(dark side)	.061±.008	.055±.005	.057±.004	.048±.002	.053±.007	.046±.005
β(bright side)	.035±.003	.031±.003	.030±.003	.032±.003	.029±.003	.031±.003
μ_2 (dark) (mag)	1.13±.10	1.14±.04	1.12±.04	1.15±.03	1.05±.08	1.07±.04
μ_2 (bright) (mag)	0.72±.04	0.73±.03	0.71±.03	0.72±.03	0.67±.02	0.71±.02
μ_2 (total) (mag)	1.85±.14	1.87±.07	1.83±.07	1.87±.06	1.72±.10	1.78±.06

Table 11. Iapetus: derived light-curve parameters. See text for details.

Table 12.

V magnitudes and colors of standard stars and of satellites.

Object	HR No.	V	u-y	v-y	b-y	r'-y	i'-y
37 Tau	1256	4.39	3.282	1.751	0.644	0.00*	0.00*
47 Tau	1311	4.86	2.545	1.268	0.501	0.07	0.13
64 Tau	1380	4.46	1.644	0.372	0.081	0.33	0.69
68 Tau	1389	4.32	1.492	0.233	0.020	0.37	0.77
ρGem	2852	4.18	1.565	0.583	0.214	0.24	0.48
₀Vir	4608	4.14	2.780	1.550	0.590	0.02	0.03
29 Psc	9087	5.14	0.544	0.004	-0.041	0.44	0.92
Titan	-	8.34	3.218	1.887	0.882	-0.05	0.11
Rhea	-	9.67	2.300	1.193	0.485	0.11	0.23
Dione	-	10.38	2.182	1.153	0.435	0.11	0.26
Tethys	-	10.22	2.131	1.123	0.455	0.15	0.24
Iapetus	-	10.96	2.145	1.105	0.426	0.07	0.19

* By definition

Table 13.

Mean opposition V magnitudes.

Satellite	V	V_o (Harris)	V_o (Blanco & Catalano)
Titan	8.34	8.39	8.35
Rhea	9.67	9.76	9.73
Dione	10.38	10.44	
Tethys	10.22	10.27	
Iapetus	10.96		

Table 14.

Solar colors in the r' and i' filters, relative to 37 Tau.

	64 Tau	68 Tau	ρ Gem	o Vir	29 Psc	Average
$(r'-y)_\odot$	+0.07	+0.07	+0.06	+0.10	+0.07	+0.07 ± .01
$(i'-y)_\odot$	+0.23	+0.22	+0.15	+0.22	+0.22	+0.21 ± .02

Table 15.

Solar Colors, Satellite Colors Relative to the Sun, and Normalized Satellite Geometric Albedos.

	Δ(u-y)	P_u	Δ(v-y)	P_v	Δ(b-y)	P_b	Δ(r'-y)	$P_{r'}$	Δ(i'-y)	$P_{i'}$
Sun	2.03±.04		1.03±.02		0.41±.01		0.07±.01		0.21±.02	
Titan	1.19	0.34	0.86	0.45	0.47	0.65	-0.12	1.12	-0.10	1.10
Rhea	0.27	0.78	0.16	0.86	0.08	0.93	0.04	0.96	0.02	0.98
Dione	0.15	0.87	0.12	0.90	0.03	0.97	0.04	0.96	0.05	0.95
Tethys	0.10	0.91	0.09	0.92	0.05	0.95	0.08	0.93	0.03	0.97
Iapetus	0.12	0.90	0.08	0.93	0.02	0.98	0.00	1.00	-0.02	1.02